Title: Inhibition of cAMP response element binding protein reduces neuronal excitability and plasticity, and triggers neurodegeneration

Running title: CREB control of neuronal survival and plasticity

Authors and author addresses: Dragana Jancic[1], Mikel Lopez de Armentia[1], Luis M. Valor, Roman Olivares and Angel Barco

Instituto de Neurociencias de Alicante (Universidad Miguel Hernández-Consejo Superior de Investigaciones Científicas). Campus de Sant Joan. Apt. 18. Sant Joan d'Alacant, 03550, Alicante, Spain

[1]These two authors contributed equally to this article

Corresponding author: Angel Barco. Instituto de Neurociencias de Alicante. Campus de Sant Joan. Apt. 18. Sant Joan d'Alacant, 03550, Alicante, Spain. Phone: +34 965 919232. Fax: +34 965 919492. Email: abarco@umh.es

Abstract

The cAMP responsive element binding protein (CREB) pathway has been involved in two major cascades of gene expression regulating neuronal function. The first one presents CREB as a critical component of the molecular switch that control long-lasting forms of neuronal plasticity and learning. The second one relates CREB to neuronal survival and protection. To investigate the role of CREB-dependent gene expression in neuronal plasticity and survival *in vivo*, we generated bitransgenic mice expressing A-CREB, an artificial peptide with strong and broad inhibitory effect on the CREB family, in forebrain neurons in a regulatable manner. The expression of A-CREB in hippocampal neurons impaired L-LTP, reduced intrinsic excitability and the susceptibility to induced seizures, and altered both basal and activity-driven gene expression. In the long-term, the chronic inhibition of CREB function caused severe loss of neurons in the CA1 subfield as well as in other brain regions. Our experiments confirmed previous findings in CREB deficient mutants and revealed new aspects of CREB-dependent gene expression in the hippocampus supporting a dual role for CREB-dependent gene expression regulating intrinsic and synaptic plasticity and promoting neuronal survival.

Keywords: CREB, neurodegeneration, synaptic plasticity, neuronal excitability, activity driven gene expression

The activation of the cAMP responsive element binding protein (CREB) pathway has been involved in two major cascades of gene expression regulating neuronal function. The first one presents CREB as a critical component of the molecular switch that control neuronal plasticity by regulating the expression of genes necessary for the formation of new synapses and the strengthening of existing synaptic connections (Josselyn and Nguyen, 2005; Kandel, 2001; Lonze and Ginty, 2002). However, the LTP and memory deficits originally reported for CREB hypomorphic mutants (mice homozygous for a deletion of the α and δ isoforms (Bourtchuladze et al., 1994)) has been found to be sensitive to gene dosage and genetic background, and the mild or absent phenotypes in hippocampal LTP and hippocampus-dependent memory observed in other CREB deficient strains have raised questions regarding the relevance of CREB in plasticity and memory (Balschun et al., 2003; Gass et al., 1998; Rammes et al., 2000). More recently, CREB has been also involved in the regulation of intrinsic plasticity in different neuronal types (Dong et al., 2006; Han et al., 2006; Huang et al., 2008; Lopez de Armentia et al., 2007).

The second gene expression cascade relates CREB to neuronal survival and protection through the transcriptional control of neurotrophins and antiapoptotic genes (Lonze and Ginty, 2002; Papadia et al., 2005; Riccio et al., 1999). Studies on $CREB^{-/-}$ mice revealed massive loss of neurons in the peripheral nervous system that caused the death of the newborn shortly after birth, whereas most neurons in the central nervous system (CNS) were not affected by CREB depletion (Lonze et al., 2002; Parlato et al., 2006). In contrast, double mutants for CREB and CREM (cAMP response element modulator) exhibited a marked and progressive cell loss in specific CNS structures, such as cortex, hippocampus and striatum (Mantamadiotis et al., 2002). This loss of neurons has not been observed in transgenic lines expressing

CREB dominant negative mutants (Kida et al., 2002; Pittenger et al., 2002; Rammes et al., 2000), likely because the time window and/or the level of CREB inhibition achieved in loss-of-function studies using gene targeting or transgenesis-based strategies were different.

The comparison of different CREB-deficient mouse strains has left important open questions concerning the role of CREB in neuronal plasticity and survival since these roles have never been investigated in parallel in the same mutant strain. We describe here a novel bitransgenic strain in which it is possible to repress in a regulated manner CREB-dependent gene expression through expression of a strong dominant negative variant of CREB known as A-CREB. This variant, which was constructed by fusing an acidic amphipathic extension onto the N-terminus of the CREB leucine zipper region, binds with very high affinity and specificity to the members of the CREB family (CREB, CREM and ATF1) blocking their binding to CRE sites (Ahn et al., 1998; Olive et al., 1997). We found that, at early times, the inhibition of this genetic cascade impaired L-LTP, reduced intrinsic neuronal excitability and the susceptibility to induced seizures, altered basal transcription, and had a relatively modest effect on activity driven gene expression. In the long-term, the sustained expression of A-CREB caused neuronal loss in the CA1 subfield of the hippocampus and other brain regions.

Materials and Methods

Generation and maintenance of transgenic mice

The DNA fragment encoding A-CREB (Ahn et al., 1998) was subcloned in the plasmid pMM400 (Mayford et al., 1996) and the NotI fragment containing A-CREB downstream of the *tetO* promoter was injected into mouse oocytes. We selected line

tetO-A-CREB-95 mice for further studies, which was backcrossed to C57BL6 F1/J mice more than eight times. We referred as A-CREB mice those bitransgenic animals that result of the crossing of *pCaMKII*-tTA mice (line B, (Mayford et al., 1996) and line *tetO*-A-CREB-95. A-CREB mice were usually raised without dox. Transgene repression was achieved by dox administration (40 mg/Kg of food) for at least one week. VP16-CREB^{high} mice have been described before (Barco et al., 2002). Mice were genotyped by PCR using the oligonucleotides pMM400-3404: AGCTCGTTTAGTGAACCGTCAGAT; pMM400-3548r: CCTCGCAGACAGCGAATTCTA; and CamKII3´end2: TTGTGGACTAAGTTTGTTCGCATC. The PCR reaction starts at 94ºC for 2min and has 35 cycles: 94ºC for 45 sec, 60.5ºC for 25 sec and 72ºC for 3min. This reaction allows the simultaneous identification of both the *pCaMKIIα*-tTA transgene (450 bp band) and the *tetO*-A-CREB transgene (150 bp band). In all our experiments, we used as control littermates mice carrying either no transgene or the tTA or *tetO* transgene alone. Mice were maintained and bred under standard conditions consistent with national guidelines and approved by the Institutional Animal Care and Use Committee.

Electrophysiology

Extracellular activity and whole cell recordings were made from acute hippocampal slices as described (Lopez de Armentia et al., 2007). XE 991 dihydrochloride (Tocris) 10 μM was bath applied for 5 minutes to ensure a complete block of I_M current. LTP experiments were performed as previously described (Barco et al., 2002).

Kindling

Five weeks old A-CREB and control littermates (n=6 in both groups) were intraperitoneally injected with subconvulsive dosage of pentylentetrazole (50mg/kg,

dissolved in saline) for several consecutive days. In the case of VP16-CREB^{high} mice, dox was removed from mouse diet one week prior to the start of the kindling experiment. The behavioural responses to the drug were classified according to the modified Racine scale (Pavlova et al., 2006): 0: no response; 1: facial automatism, with twitching of the ears and whiskers; 2: convulsive waves propagating along the axis of the trunk; 3: myoclonic convulsions with rearing; 4: clonic convulsions with loss of posture; and 5: repeated, forceful, clonic-tonic or lethal convulsions. All subjects were monitored for at least 20 minutes after the injection and scored.

Histological techniques

Nissl and immunohistochemistry stainings were performed as previously described (Lopez de Armentia et al., 2007). In cell counting experiments, cerebral cortex, CA1 pyramidal layer and DG granular cells layer thickness were counted from 50-µm coronal brain sections from ≥6 months old A-CREB (n=7) and their wildtype littermates (n=6) in a Leica microscope. For each animal, 3 sections were Nissl-stained and cells were counted in 5 defined regions and analyzed using Image-J software. α-M2-flag, α-Synaptophysin, α-MAP-2, α-Calbindin, α-GAP-43 and secondary antibodies were obtained from Sigma; α-CREB antibodies were purchased to Cell Signaling; and α-CREM antiserum was a gift from Günther Schütz's lab. *In situ* hybridizations were performed as previously described using appropriate cRNA probes labelled with digoxigenin (Shumyatsky et al., 2002).

Quantitative RT-PCR

qPCR was carried out in an Applied Biosystems 7300 real-time PCR unit using *SYBR* mix (Invitrogen) and primers specific for Arc, BDNF, c-Fos, CREM, the N-terminus of CREB and GADPH. Each independent sample was assayed in duplicate and normalized using GAPDH levels.

Microarray analysis

RNA was extracted from dissected hippocampi. Mouse Genome 430 2.0 genechips were hybridized, stained, washed and screened for quality according to the manufacturer's protocol. The Affymetrix GeneChip® data were processed, normalized and statistically analyzed using GCOS (Affymetrix), GeneSpring GX (Agilent Technologies) and dChip softwares (Li and Hung Wong, 2001). This dataset will be accessible at the GEO database. See additional details in Supplementary Methods.

Behavioral analysis

For all behavioral tasks, we used adult male mutant and control littermates. The battery of behavioral tasks was initiated when the animals were 2 months old and finished when they were 4 months old. The experimenter was blind to genotypes. *SHIRPA primary screen:* Mice were evaluated using a modification of Irwin procedure (Irwin, 1968). *Open field:* Mice were placed in 50×50 cm^2 open-field chambers and monitored throughout the test session (30 min) by a video-tracking system (SMART, Panlab S.L., Barcelona, Spain), which records the position of each animal every 0.5 sec. *Water Maze:* The visible and hidden platform tasks were carried out in a 170 cm pool using SMART software (Panlab S.L.). Four training trials, 120 s maximum and 30-100 min ITI (inter-trial interval) were given daily. Probe trials (60 s) were performed to assess retention of the previously acquired information. Further detail on procedures can be found in (Viosca et al., 2008).

Results

Regulated expression of A-CREB in forebrain neurons

To investigate the consequences of impaired CREB-dependent gene expression in neuronal survival and function, we generated transgenic mice expressing the strong

repressor of CRE-binding activity A-CREB. We used the CamKIIα-tTA system of inducible transgenics to restrict the expression to forebrain neurons (Mayford et al., 1996) (Fig. 1A). We focused our research on the role of CREB-dependent gene expression in hippocampal function in the bitransgenic strain CamKIIα-tTA/AC95, from now on referred as A-CREB mice, which showed the strongest expression in this brain region. The expression of A-CREB mRNA in this strain was restricted to specific layers of the cerebral cortex, the striatum and the hippocampus, preferentially in the CA1 field, although scattered positive cells were also detected in the dentate gyrus (Fig. 1B-C and Supplementary Fig. S1). Western-blot and immunohistochemistry analyses using anti-M2 Flag antibody, which recognizes A-CREB, demonstrated the efficient translation of the transgene (Fig. 1D and Supplementary Fig. S1B). The expression of A-CREB did not affect the level of CREB mRNA (Fig. 1E). However, in agreement with recent studies *in vitro* (Mouravlev et al., 2007), dimerization with A-CREB promoted CREB degradation as evidenced by the decrease of CREB immunoreactivity in the CA1 subfield (Fig. 1F).

We assayed the efficacy of doxycycline (dox) to regulate transgene expression. As expected, we found that addition of dox to the mouse diet turned off transgene expression in less than two weeks (Fig. 1G). In contrast, the opposite manipulation, turning on transgene expression in mice in which it was turned off during embryonic and early postnatal development, failed to show efficient transgene induction (Fig. 1H). This result is in agreement with the recent report by Zhu and colleagues showing that tetO constructs, when turned off during embryonic development, are some times irreversibly silenced (Zhu et al., 2007).

Chronic expression of A-CREB causes neuronal loss in hippocampus and cortex

A-CREB and control littermates were undistinguishable during the first postnatal weeks and had a normal life span. However, mutant mice did not gain as much weight as their control littermates suggesting some deleterious effect of A-CREB expression (Fig. 2A). *In situ* hybridization analysis of transgene expression at different ages revealed a progressive reduction on the level of expression of A-CREB mRNA in the hippocampus (Fig. 2B). The analysis of hippocampal anatomy in these sections suggested that this reduction on transgene expression was largely due to the death of neurons that expressed the transgene (Figs. 2C, 2D and Supplementary Fig. S2). The neurodegenerative process progressed during several weeks and halted at later times, in which we could not longer detect the expression of the transgene in the CA1 area. The thickness of both the CA1 *stratum pyramidale* and cortex were severely reduced in adult A-CREB mice (Fig. 2D). Mice that expressed the transgene for several months still showed strong expression in cortical layers, indicating that those neurons may be more resistant to the chronic inhibition of CREB function than CA1 neurons (Fig. 2D and Supplementary Fig. S1C). Interestingly, it was possible to stop and reinitiate the degenerative process by turning off and on transgene expression in adult animals (Fig. 2E). A-CREB animals raised in the presence of dox did not express the transgene and therefore did not show cell loss (results not shown).

Severe loss of CA1 neurons has been also observed in CREB/CREM double knockout mice (Mantamadiotis et al., 2002). This might suggest that the disruption of CREB signaling in A-CREB mice was comparable to that in CREB/CREM double knockouts and likely more dramatic than that achieved in previous transgenic approaches. We then proceeded to re-evaluate in this strain some of the open questions concerning the role of CREB on hippocampal L-LTP and neuronal survival, as well as to assess novel aspects of CREB function, such as regulation of intrinsic

excitability in CA1 pyramidal neurons and susceptibility to seizure. Although we primarily focused on the early effects of CREB inhibition in hippocampal physiology and gene expression prior to neuronal damage (Figs. 3-6), we also explored the late consequences of the sustained inhibition of CREB function and the severe cell loss (Fig. 7).

Inhibition of CREB activity impairs L-LTP

Loss and gain-of-function studies have suggested a role for CREB in the late phase of LTP in the Schaffer collateral pathway. However, the absence of a clear phenotype in LTP studies on some CREB deficient strains has raised questions regarding the relevance of CREB in hippocampal plasticity. These discrepancies may be due to compensatory effects between different CRE-binding proteins. Unfortunately, L-LTP has not been assessed in CREB/CREM double knockout mice. To clarify this issue, we examined synaptic plasticity in the Schaffer collateral pathway of 3 weeks old A-CREB mice, a time at which no neuronal damage was detected. Field recordings in acute hippocampal slices from A-CREB mice did not reveal abnormalities in basal synaptic transmission (Fig. 3A and 3B) or alterations in spontaneous activity at the CA1 subfield (Fig. 3C). E-LTP in response to one standard 100 Hz tetanus train of 1 sec duration was also normal (Fig. 3D). However, in agreement with previous studies in CREB deficient mutants (Bourtchuladze et al., 1994), L-LTP in response to four tetani was impaired after 2 hours (Fig. 3E, 200-240 min: A-CREB: 122±1 %, n=10 (8); WT: 163±1 %, n=12 (8); $p<0.001$).

Inhibition of CREB activity reduces neuronal excitability and delays kindling

Enhanced CREB activity in CA1 pyramidal neurons increased intrinsic excitability and the spontaneous activity of hippocampal circuits (Lopez de Armentia et al.,

2007). To investigate whether opposite changes occurred after inhibition of CREB function, we examined the intrinsic properties of CA1 neurons in juvenile A-CREB mice. Intracellular recordings in CA1 pyramidal neurons of three weeks old mutant mice revealed that the expression of A-CREB significantly reduced the number of action potentials (APs) elicited by depolarizing current injections (Fig. 4A and 4B; $p< 0.001$). We also observed that rehobase current to elicit an AP was bigger in A-CREB mice due to a reduction in membrane resistance (Supplementary Table 1 and Fig. 4C). Since we observed differences in the amplitude of the fast but not in the slow component of the AHP, we tested whether the decrease of membrane resistance was produced by an increase of the M potassium current (Storm, 1989). The selective M-channel blocker XE-991 (Wang et al., 1998) reversed the membrane resistance and rehobase differences between A-CREB and control mice (Fig. 4D and Supplementary Table 1) suggesting that an enhancement in the M current may underlay the decrease in intrinsic excitability. The reduction of intrinsic excitability (Fig. 4B; $p=0.30$) and the differences in resistance and rehobase (Fig. 4E, Supplementary Table 1) were also reversed when transgene expression was repressed for 10 days with dox.

We recently reported that strong chronic increase of CREB activity, when sustained for several weeks, triggered the occurrence of sporadic seizures that often caused the animal death (Lopez de Armentia et al., 2007). In contrast, A-CREB mice had a normal life span and we never observed spontaneous epileptic seizures. In fact, our findings in CA1 neurons physiology suggested that A-CREB mice could be resistant to induced epilepsy. To assess this hypothesis, we repeatedly injected mice with the pro-epileptic drug pentylenetetrazol (PTZ) at subconvulsive concentration. In control mice, daily injection for 10 days was sufficient to induce kindling in all individuals. In contrast, A-CREB mice exhibited delayed kindling and needed several

additional subconvulsive injections of PTZ to show seizure (Fig. 5A). Interestingly, we carried out the same experiment in the transgenic strain with chronic enhancement of CREB function (VP16-CREB^{high} mice) and obtained the opposite result: whereas reduced CREB activity delayed kindling, enhanced CREB activity accelerated it (Fig. 5B). These results indicate that CREB can control neuronal responsiveness in both directions promoting and attenuating intrinsic excitability and plasticity.

A-CREB expression causes transcriptional alterations

To evaluate the early transcriptional effects of CREB inhibition by A-CREB, we compared the profiles of gene expression in the hippocampus of three weeks old transgenic and control mice using *Affymetrix* microarrays MouseArray 430 2.0. Since we were interested in activity driven gene expression, we compared both genotypes in the basal condition and 2 hours after kainate-induced seizures. We observed that, in agreement with previous observations during kindling experiments, A-CREB mice were more resistant to seizures than their control siblings. The same dose of kainate elicited less severe seizures in mutant mice, as determined by forelimbs clonus, rearing and falling, and death (Fig. 6A). The reduced susceptibility to KA can obviously interfere with our analysis of activity driven gene expression. For this reason, we obtained samples corresponding to five different conditions: control mice (WT), control mice injected with 14 mg/Kg of KA (seizure >4), A-CREB mice, A-CREB mice injected with 14 mg/Kg of KA (seizure <4), and A-CREB mice injected with 18 mg/Kg of KA (seizure >4).

The screen for genes specifically affected by A-CREB expression in the basal state revealed both downregulated and upregulated probe sets (Cluster 1 and 2 respectively in Fig. 6B, see also Supplementary Table 2). The largest fold changes (FC) in the short list of genes consistently downregulated in A-CREB mutants, both

in mice injected with saline or with kainate, corresponded to *scn4b* and *penk1* probe sets. *Scn4b* encodes the sodium channel subunit β4, which has been recently identified as significantly downregulated in Huntington's disease patients and in pre- and post symptomatic mouse model for this condition (Oyama et al., 2006). *Penk1* encodes proenkephalin, an important neuropeptide previously identified as a direct target of CREB in striatal neurons *in vivo* (Konradi et al., 1993; Pittenger et al., 2002). For upregulated genes, the biggest change corresponded to two probe sets targeted to *Trat1* encoding the T cell receptor associated transmembrane adaptor 1, whose role in neurons remains unexplored. As expected, we also observed strong increase of the signal of the two probes complementary to A-CREB sequence (Fig. 6C).

The screen for genes specifically affected by seizure revealed a large number of strongly upregulated genes (FC>4) and a few modestly downregulated genes (FC<2). The group of upregulated genes included a number of previously identified immediate early genes (IEGs), such as those encoding the transcription factors c-Fos, FosB, c-Jun, Egr-1, Egr-2, Egr-3, the neurotrophin BDNF, the cytoskeletal protein Arc and others, which represent the initial nuclear response to the activation of intracellular signaling cascades by synaptic activity and may play important roles on neuronal survival and synaptic plasticity (Tischmeyer and Grimm, 1999). Many IEGs have CRE sites in their promoters and are thought to be regulated by CREB. In fact, many IEGs were found upregulated in mice with chronic enhancement of CREB function (Barco et al., 2005). Strikingly, we found that the induction of most IEGs was not affected by A-CREB expression (Fig. 6D-E, Table 1 and Supplementary Table 3), indicating that, although CREB activity is sufficient for the expression of many IEGs, it was not necessary for their induction in response to kainate. More detailed analyses revealed mild deficiencies in the basal expression of some important

activity-dependent genes, such as *egr1*, *egr2*, a possible isoform of Homer 1 (*C330006P03Rik*) and *arc* (Supplementary Table 4), that were not initially detected, probably due to the stringency of the two-way ANOVA analysis (see Supplementary Methods for further details). However, these IEGs where still strongly upregulated by kainate in the hippocampus of A-CREB mice. The list of genes significantly altered in A-CREB mice and differentially upregulated in response to kainate in A-CREB mice was surprisingly short (Supplementary Table 2) and included *penk1* and *pdyn*, which encode for two precursors of opioid neuropeptides previously identified as CREB targets. Interestingly, *pdyn* was the gene that showed the strongest upregulation after chronic enhancement of CREB function (Barco et al., 2005).

To confirm our microarray results indicating that the induction of IEGs was not affected by A-CREB expression, we examined the expression of four representative IEGs, *fos*, *egr1*, *arc* and *bdnf*, in the hippocampus of transgenic mice using well known paradigms that trigger activity-dependent gene expression: induction of epileptic seizure by kainic acid and exploration of a novel environment. Although we confirmed the array results, we observed larger individual differences in the response to seizure in A-CREB mice than in control littermates (Fig. 6A). Induction of these four IEGs correlated well with seizure intensity in the lower range of the Racine scale (1-3). As a consequence, activity-dependent upregulation of these genes was apparently impaired in some mutant mice (Fig. 6F). This difference was likely not observed in the microarray analysis because we pooled together the hippocampi of several mice in each sample. When we used a higher dose of kainate (18 mg/Kg) strong upregulation of IEGs was consistently observed in the hippocampus of A-CREB animals (Fig. 6F, right panels). In agreement with our microarray analysis, Arc mRNA was slightly but significantly reduced in the basal

condition (Fig. 6G). Similar results were obtained in response to novelty exploration (Fig. 6H and results not shown). These results together with the microarray analysis suggest that other transcription factors can compensate the inhibition of CREB function in the control of some forms of activity-driven gene expression. Previous analyses of CREB knockout mice suggested that this compensation could be caused by the upregulation of the cAMP response element modulator (CREM) (Blendy et al., 1996; Hummler et al., 1994; Mantamadiotis et al., 2002). Neither microarray analysis (Table 2), immunostaining using an antiserum against CREM (Fig. 6I), nor qRT-PCR (Fig. 6J) revealed significant changes of CREM expression in the hippocampus of A-CREB mice at the basal stage. Since A-CREB can bind and block the activity of both CREB and CREM (Ahn et al., 1998), these results could suggest that the upregulation of CREM observed in CREB knockout mice could be mediated by CREM itself. We did not observe either upregulation of ATF1 mRNA in the hippocampus of A-CREB mice (Table 2).

Late consequences of chronic inhibition of CREB function

The neurodegeneration observed after sustained inhibition of CREB function by A-CREB had important consequences in neuronal physiology and brain function that were independent of the earlier effects of CREB inhibition described above. Thus, whereas 3 weeks old A-CREB mice did not show abnormalities in basal synaptic transmission (Fig. 3A), one-year old A-CREB mice showed a significant reduction in the response of CA1 pyramidal neurons to stimulation of afferent CA3 axons reflecting the severe loss of neurons in the CA1 subfield (Fig. 7A). We also tested adult A-CREB mice in an extensive battery of behavioral tasks and detected alterations in some basal behaviors, such as touch escape o geotaxis (Supplementary Table 5), hyperactivity in an open field (Fig. 7B), and strong impairments in spatial

navigation (Fig. 7C-D). These behavioral abnormalities are consistent with the wide spread degeneration detected at this stage.

Discussion

The multilevel analysis of A-CREB mice has allowed to address a number of important open questions concerning the role of CREB in plasticity and survival, contributing to clarify some of controversies concerning CREB loss-of-function studies. Thus, we described here the consequences in neuronal gene expression, plasticity and survival of blocking CREB-dependent gene expression and showed for the first time that the inhibition of CREB reduced the intrinsic excitability of CA1 neurons through modulation of the I_M current, an alteration that can underlay the reduced seizure susceptibility observed in A-CREB mice. In agreement with previous studies on CREB deficient mutants, we found that the chronic inhibition of CREB function reduced synaptic plasticity in the Schaffer collateral pathway and compromised neuronal viability. Moreover, we demonstrated changes in both basal and activity-induced gene expression that, despite being milder than anticipated, contributed to clarify the genetic program regulated *in vivo* by this family of transcription factors.

A novel mouse model to investigate CREB function in vivo

The bitransgenic mouse strain described here has a number of advantages for investigating the role of CREB in the adult brain. First, A-CREB mice express a stronger repressor than those used in previous studies on transgenic strains. CREB-M1, the point mutant (S133A) used in two previous studies (Kida et al., 2002; Rammes et al., 2000), cannot be phosphorylated at Ser 133 and inhibits CREB-dependent gene expression by competing with CREB for CRE sites, although it has

been shown that CREB/CREB-M1 heterodimers can still exhibit significant transactivation capability (Loriaux et al., 1993). K-CREB, the point mutant (R287L) used by Pittenger and colleagues (Pittenger et al., 2002), blocks gene activation by binding to CREB and other CREB family members and preventing their interaction with CRE sites. In contrast, A-CREB is a short polypeptide specifically designed to form highly stable heterodimers with CREB-family members. A-CREB/CREB heterodimers are formed with an affinity 3.3 orders of magnitude greater than CREB homodimers (Ahn et al., 1998) and, likely, than CREB heterodimers with K-CREB or CREB-M1 since neither one of these point mutations affects dimerization. Because of this, A-CREB may have a stronger dominant negative effect than K-CREB or CREB-M1. Studies in cell culture supports this view (Ching et al., 2004). Second, A-CREB mice are likely more adequate than CREB knockout mice to investigate the consequences of disrupting the CREB pathway. Since the leucine zipper domain of CREB has a high degree of homology with those of CREM and ATF1 and since these three proteins can form heterodimers with each other, A-CREB should have, in principle, also the capability of blocking the binding of CREM and ATF1 to DNA. Experiments in cultured cells have demonstrated this capability in the case of ATF1 and CREB (Ahn et al., 1998). The reduction of endogenous CREB detected by immunohistochemistry indicates that A-CREB can also dimerize with CREB in the brain of A-CREB mice, whereas the dramatic loss of neurons observed after sustained transgene expression suggests that both CREB and CREM may be target of A-CREB inhibition. Therefore, our transgenic approach most likely does not distinguish between the role of CREB and that of highly related ATF1 and CREM as positive mediators of CRE-driven transcription. Third, we did not detect in our model the compensatory upregulation of other ATF/CREB family members observed in CREB

hypomorphic and knockout mice. And fourth, the possibility of regulating transgene expression with dox allowed to assess the reversal of relevant phenotypes.

Bidirectional modulation of intrinsic and synaptic plasticity by CREB-mediated gene expression

Gain-of-function approaches have demonstrated that the expression of constitutively active CREB facilitates the consolidation of LTP in the Schaffer collateral pathway (Barco et al., 2002; Marie et al., 2005), suggesting that CREB activity is sufficient to sustain this process. In contrast, loss-of-function studies aimed to investigate the requirement of CREB in L-LTP produced mixed results. Whereas CREB hypomorphic mutants and transgenic mice expressing the dominant negative CREB variant K-CREB showed deficits in some forms of L-LTP (Bourtchuladze et al., 1994; Huang et al., 2004; Pittenger et al., 2002), no deficits were found in mice in which CREB was specifically depleted in forebrain neurons and in transgenic mice expressing the dominant negative CREB variant CREB-M1. These negative results might be caused by insufficient CREB inhibition (Rammes et al., 2000) or by CREM compensation (Balschun et al., 2003). A possible explanation to reconcile these studies would be that CRE-driven gene expression, but not CREB itself, is required for L-LTP in the Schaffer collateral pathway. Testing this hypothesis would require the analysis of animals in which both CREB and CREM activities are simultaneously repressed (Balschun et al., 2003). This seems to be the case in A-CREB mice. Notably, LTP analysis of 3-weeks old A-CREB mice revealed significant deficits in the late phase of LTP, supporting a role for CREB-dependent gene expression in the consolidation of some forms of LTP.

This study also provided first evidence of negative regulation of intrinsic excitability in CA1 neurons by CREB inhibition. Our analysis suggested that

modulation of M potassium current, which contributes to spike frequency activation in CA1 pyramidal neurons (Peters et al., 2005), produced a decrement in excitability, a finding that would also contribute to explain the resistance to seizure observed in A-CREB mice (this study) and ICER-overexpressing transgenics (Kojima et al., 2008). The increase in I_M current observed in CA1 neurons expressing A-CREB resembled that produced by retigabine, an M channel opener that reduces both kindled and epileptic seizures (Rostock et al., 1996). Kindling experiments in bitransgenic mice with chronic inhibition or enhancement of CREB function highlighted the relevance of accurate regulation of neuronal excitability by CREB in epilepsy. This novel, but now well-established, CREB function suggests that the activation of CREB-dependent gene expression does not only contribute to the stabilization of ongoing reinforcements of synaptic connections (consolidation), but can also facilitate future neuronal responses in a given time range (sensitization).

CREB is sufficient, but not always necessary for activity-driven gene expression

Biochemical and molecular studies have demonstrated the participation of CREB in the regulation of the expression of more than one hundred genes. The availability of complete genome sequences and the widespread application of genome-wide transcriptional profiling and binding mapping techniques have recently allowed the identification of even more potential targets (Euskirchen et al., 2004; Impey et al., 2004; Tanis et al., 2008; Zhang et al., 2005). Complementary to these assays, gene profiling of CREB mutant mice can also contribute to our understanding of the complex gene programs triggered by CREB (Barco et al., 2005; McClung and Nestler, 2003).

The transcriptional response to seizure in the hippocampus of A-CREB and control mice was remarkably similar despite the relatively weaker limbic seizures

induced by the drug in A-CREB mice and the clear effects of A-CREB expression in neuronal survival and physiology. Our analysis revealed that the presence of CRE sites in a promoter was not a good predictor of CREB requirement for its seizure-driven transcription (see Table 1 and Supplementary Tables 2-4, column 'CRE sites'), although we cannot discard that these sites could bind CREB under other circumstances. This result is in agreement with a previous study on CREB hypomorphic mice (Blendy et al., 1995) and very recent microarray analyses of activity driven gene expression in CREB/CREM double mutants (Lemberger et al., 2008).

Extensive evidence identified the CREB family of transcription factors as a major regulator of activity-dependent gene expression (Josselyn and Nguyen, 2005; Lonze and Ginty, 2002). The relatively modest transcriptional alterations observed in A-CREB mice after kainate injection might be explained by partial or insufficient inhibition of CREB activity by A-CREB. However, the progressive neurodegeneration of CA1 neurons suggested that inhibition of CREB activity in the hippocampus of A-CREB mice was as robust as in CREB/CREM double deficient mutants, which, notably, also showed normal activity-driven gene expression in response to kainate (Lemberger et al., 2008). Another possible explanation would be the compensation by other members of the CREB family, but again the results in CREB/CREM double deficient mutants and the absence of changes in CREM and ATF1 expression in A-CREB mice (Table 2) suggested that this is not likely the case. However, we cannot completely discard that alternate CRE-binding factors may escape A-CREB inhibition. A third explanation would be that the induction of IEGs by kainate is not mediated solely by CREB and CREs. The promoter region of many IEGs contain binding site for other activity-dependent transcription factors. Mice

deficient in the serum response factor (SRF), the main transcription factor binding to the SRE sites also located in the promoter of many IEGs, showed a profound defect in activity-dependent IEG expression, indicating that activity-dependent gene expression in response to epileptic activity may be primarily regulated by this transcription factor rather than by CREB (Ramanan et al., 2005). This does not mean that CREB does not contribute to activity-driven gene expression. On the contrary, CREB/CREM activity seems to be required for most of the cocaine-induced expression changes in the striatum (Lemberger et al., 2008). Moreover, previous studies have shown that CREB contributes to the regulation of important IEGs, such as *bdnf*, *c-fos*, and *JunB*, also in the hippocampus. CREB can even be sufficient for their expression (Barco et al., 2005), but it appears to be not always necessary. In contrast, CREB was not sufficient to trigger *arc* expression (Barco et al., 2005), but we found now that it is necessary to achieve normal levels of basal expression. Future chromatin occupancy experiments on prototypical IEG promoters may clarify the role of CREB in constitutive and activity-driven neuronal gene expression *in vivo*.

The microarray analysis revealed transcriptional changes that can be highly relevant to explain the phenotype of A-CREB mice. Thus, genes that are known to play critical roles in epileptogenesis, excitability and plasticity were reduced in the basal condition (*arc*, *egr1*, *egr2*), or in response to kainate (*penk*, *pdyn)*. Furthermore, the confluence of diverse subtle changes in gene expression may promote a cascade of summatory events that led to robust phenotypical effects. Further research should determine the precise molecular links between the altered expression patterns and the reduced neuronal excitability and impaired plasticity observed at early times, and the neuronal loss observed at later times.

CREB-dependent gene expression is required for the survival of CA1 neurons

The analysis of the hippocampus of A-CREB mice revealed massive loss of neurons in the CA1 subfield, likely as a consequence of the dramatic and substained inhibition of CREB function in pyramidal neurons. The neurodegenerative process observed in A-CREB mice presented some similarities with that described for *Creb1*^{Camkcre4}*Crem*$^{-/-}$ double mutants (Mantamadiotis et al., 2002), suggesting that both CREB and CREM function were effectively blocked by A-CREB expression.

Gene profiling analysis of A-CREB mice did not reveal significant downregulation of some CREB target genes involved in promoting neuronal survival, such as *bcl-2* and *bdnf*, but identified other genes whose upregulation or downregulation in the basal state may contribute to explain the neurodegenerative process, for instance, *Scn4b*, the cell death-related genes *Cst7* and *Cxcl10* and several genes induced by interferon. These changes may represent an early transcriptional signature preceding neurodegeneration. There may also exist a causal relationship between the early physiological alterations – reduced neuronal excitability and impaired plasticity – and the late pathological events. Lower than normal neuronal activity can, in the long-term, cause the loss of neurons in hippocampal circuits, especially in juvenile animals (Kaindl et al., 2006).

The ability to pause and reactivate neurodegeneration using doxycycline makes the transgenic strain described here a powerful animal model to assay therapies aimed to compensate deficiencies in the cAMP signaling pathway, which has been critically involved in Hungtinton's and Alzheimer's disease neurodegeneration (Sugars et al., 2004; Vitolo et al., 2002).

Funding: Research at AB's lab is supported by the European Commission grants MEXT-CT-2003-509550 and MIRG-CT2005-016343, Spanish MEC Grants BFU2005-00286 and CSD2007-00023, and grants from Fundació La Marató de TV3 and Fundación Ramón Areces.

Acknowledgments: The authors thank Eloisa Herrera, Rafael Lujan, Eric R. Kandel and members of Barco's lab for critical reading of the manuscript and helpful comments. We also thank Eric R. Kandel, Yan-you Huang and other members of Kandel's lab for their support and help in the generation and early experiments with A-CREB mice. The assistance and advice of Jose Viosca during the behavioral analysis of A-CREB mice is also acknowledged.

Corresponding author: Angel Barco. Instituto de Neurociencias de Alicante. Campus de Sant Joan. Apt. 18. Sant Joan d'Alacant, 03550, Alicante, Spain. Phone: +34 965 919232. Fax: +34 965 919492. Email: abarco@umh.es

References

Ahn S, Olive M, Aggarwal S, Krylov D, Ginty DD, Vinson C. 1998. A dominant-negative inhibitor of CREB reveals that it is a general mediator of stimulus-dependent transcription of c-fos. Mol Cell Biol. 18:967-977.

Balschun D, Wolfer DP, Gass P, Mantamadiotis T, Welzl H, Schutz G, Frey JU, Lipp HP. 2003. Does cAMP response element-binding protein have a pivotal role in hippocampal synaptic plasticity and hippocampus-dependent memory? J Neurosci. 23:6304-6314.

Barco A, Alarcon JM, Kandel ER. 2002. Expression of constitutively active CREB protein facilitates the late phase of long-term potentiation by enhancing synaptic capture. Cell. 108:689-703.

Barco A, Patterson S, Alarcon JM, Gromova P, Mata-Roig M, Morozov A, Kandel ER. 2005. Gene Expression Profiling of Facilitated L-LTP in VP16-CREB Mice Reveals that BDNF Is Critical for the Maintenance of LTP and Its Synaptic Capture. Neuron. 48:123-137.

Blendy JA, Kaestner KH, Schmid W, Gass P, Schutz G. 1996. Targeting of the CREB gene leads to up-regulation of a novel CREB mRNA isoform. Embo J. 15:1098-1106.

Blendy JA, Schmid W, Kiessling M, Schutz G, Gass P. 1995. Effects of kainic acid induced seizures on immediate early gene expression in mice with a targeted mutation of the CREB gene. Brain Res. 681:8-14.

Bourtchuladze R, Frenguelli B, Blendy J, Cioffi D, Schutz G, Silva AJ. 1994. Deficient long-term memory in mice with a targeted mutation of the cAMP-responsive element-binding protein. Cell. 79:59-68.

Ching YP, Chun AC, Chin KT, Zhang ZQ, Jeang KT, Jin DY. 2004. Specific TATAA and bZIP requirements suggest that HTLV-I Tax has transcriptional activity subsequent to the assembly of an initiation complex. Retrovirology. 1:18.

Dong Y, Green T, Saal D, Marie H, Neve R, Nestler EJ, Malenka RC. 2006. CREB modulates excitability of nucleus accumbens neurons. Nat Neurosci. 9:475-477.

Euskirchen G, Royce TE, Bertone P, Martone R, Rinn JL, Nelson FK, Sayward F, Luscombe NM, Miller P, Gerstein M, Weissman S, Snyder M. 2004. CREB binds to multiple loci on human chromosome 22. Mol Cell Biol. 24:3804-3814.

Gass P, Wolfer DP, Balschun D, Rudolph D, Frey U, Lipp HP, Schutz G. 1998. Deficits in memory tasks of mice with CREB mutations depend on gene dosage. Learn Mem. 5:274-288.

Han MH, Bolanos CA, Green TA, Olson VG, Neve RL, Liu RJ, Aghajanian GK, Nestler EJ. 2006. Role of cAMP response element-binding protein in the rat locus ceruleus: regulation of neuronal activity and opiate withdrawal behaviors. J Neurosci. 26:4624-4629.

Huang YH, Lin Y, Brown TE, Han MH, Saal DB, Neve RL, Zukin RS, Sorg BA, Nestler EJ, Malenka RC, Dong Y. 2008. CREB modulates the functional output of nucleus accumbens neurons: a critical role of N-methyl-D-aspartate glutamate receptor (NMDAR) receptors. J Biol Chem. 283:2751-2760.

Huang YY, Pittenger C, Kandel ER. 2004. A form of long-lasting, learning-related synaptic plasticity in the hippocampus induced by heterosynaptic low-frequency pairing. Proc Natl Acad Sci U S A. 101:859-864.

Hummler E, Cole TJ, Blendy JA, Ganss R, Aguzzi A, Schmid W, Beermann F, Schutz G. 1994. Targeted mutation of the CREB gene: compensation within the CREB/ATF family of transcription factors. Proc Natl Acad Sci U S A. 91:5647-5651.

Impey S, McCorkle SR, Cha-Molstad H, Dwyer JM, Yochum GS, Boss JM, McWeeney S, Dunn JJ, Mandel G, Goodman RH. 2004. Defining the CREB regulon: a genome-wide analysis of transcription factor regulatory regions. Cell. 119:1041-1054.

Irwin S. 1968. Comprehensive observational assessment: Ia. A systematic, quantitative procedure for assessing the behavioral and physiologic state of the mouse. Psychopharmacologia. 13:222-257.

Josselyn SA, Nguyen PV. 2005. CREB, synapses and memory disorders: past progress and future challenges. Curr Drug Targets CNS Neurol Disord. 4:481-497.

Kaindl AM, Asimiadou S, Manthey D, Hagen MV, Turski L, Ikonomidou C. 2006. Antiepileptic drugs and the developing brain. Cell Mol Life Sci. 63:399-413.

Kandel ER. 2001. The molecular biology of memory storage: a dialogue between genes and synapses. Science. 294:1030-1038.

Kida S, Josselyn SA, de Ortiz SP, Kogan JH, Chevere I, Masushige S, Silva AJ. 2002. CREB required for the stability of new and reactivated fear memories. Nat Neurosci. 5:348-355.

Kojima N, Borlikova G, Sakamoto T, Yamada K, Ikeda T, Itohara S, Niki H, Endo S. 2008. Inducible cAMP early repressor acts as a negative regulator for kindling epileptogenesis and long-term fear memory. J Neurosci. 28:6459-6472.

Konradi C, Kobierski LA, Nguyen TV, Heckers S, Hyman SE. 1993. The cAMP-response-element-binding protein interacts, but Fos protein does not interact, with the proenkephalin enhancer in rat striatum. Proc Natl Acad Sci U S A. 90:7005-7009.

Lemberger T, Parkitna JR, Chai M, Schutz G, Engblom D. 2008. CREB has a context-dependent role in activity-regulated transcription and maintains neuronal cholesterol homeostasis. Faseb J.

Li C, Hung Wong W. 2001. Model-based analysis of oligonucleotide arrays: model validation, design issues and standard error application. Genome Biol. 2:RESEARCH0032.

Lonze BE, Ginty DD. 2002. Function and regulation of CREB family transcription factors in the nervous system. Neuron. 35:605-623.

Lonze BE, Riccio A, Cohen S, Ginty DD. 2002. Apoptosis, axonal growth defects, and degeneration of peripheral neurons in mice lacking CREB. Neuron. 34:371-385.

Lopez de Armentia M, Jancic D, Olivares R, Alarcon JM, Kandel ER, Barco A. 2007. cAMP response element-binding protein-mediated gene expression increases the intrinsic excitability of CA1 pyramidal neurons. J Neurosci. 27:13909-13918.

Loriaux MM, Rehfuss RP, Brennan RG, Goodman RH. 1993. Engineered leucine zippers show that hemiphosphorylated CREB complexes are transcriptionally active. Proc Natl Acad Sci U S A. 90:9046-9050.

Mantamadiotis T, Lemberger T, Bleckmann SC, Kern H, Kretz O, Martin Villalba A, Tronche F, Kellendonk C, Gau D, Kapfhammer J, Otto C, Schmid W, Schutz G. 2002. Disruption of CREB function in brain leads to neurodegeneration. Nat Genet. 31:47-54.

Marie H, Morishita W, Yu X, Calakos N, Malenka RC. 2005. Generation of silent synapses by acute in vivo expression of CaMKIV and CREB. Neuron. 45:741-752.

Mayford M, Bach ME, Huang YY, Wang L, Hawkins RD, Kandel ER. 1996. Control of memory formation through regulated expression of a CaMKII transgene. Science. 274:1678-1683.

McClung CA, Nestler EJ. 2003. Regulation of gene expression and cocaine reward by CREB and DeltaFosB. Nat Neurosci. 6:1208-1215.

Mouravlev A, Young D, During MJ. 2007. Phosphorylation-dependent degradation of transgenic CREB protein initiated by heterodimerization. Brain Res. 1130:31-37.

Olive M, Krylov D, Echlin DR, Gardner K, Taparowsky E, Vinson C. 1997. A dominant negative to activation protein-1 (AP1) that abolishes DNA binding and inhibits oncogenesis. J Biol Chem. 272:18586-18594.

Oyama F, Miyazaki H, Sakamoto N, Becquet C, Machida Y, Kaneko K, Uchikawa C, Suzuki T, Kurosawa M, Ikeda T, Tamaoka A, Sakurai T, Nukina N. 2006. Sodium channel beta4 subunit: down-regulation and possible involvement in neuritic degeneration in Huntington's disease transgenic mice. J Neurochem. 98:518-529.

Papadia S, Stevenson P, Hardingham NR, Bading H, Hardingham GE. 2005. Nuclear Ca2+ and the cAMP response element-binding protein family mediate a late phase of activity-dependent neuroprotection. J Neurosci. 25:4279-4287.

Parlato R, Rieker C, Turiault M, Tronche F, Schutz G. 2006. Survival of DA neurons is independent of CREM upregulation in absence of CREB. Genesis. 44:454-464.

Pavlova T, Stepanichev M, Gulyaeva N. 2006. Pentylenetetrazole kindling induces neuronal cyclin B1 expression in rat hippocampus. Neurosci Lett. 392:154-158.

Peters HC, Hu H, Pongs O, Storm JF, Isbrandt D. 2005. Conditional transgenic suppression of M channels in mouse brain reveals functions in neuronal excitability, resonance and behavior. Nat Neurosci. 8:51-60.

Pittenger C, Huang YY, Paletzki RF, Bourtchouladze R, Scanlin H, Vronskaya S, Kandel ER. 2002. Reversible inhibition of CREB/ATF transcription factors in region CA1 of the dorsal hippocampus disrupts hippocampus-dependent spatial memory. Neuron. 34:447-462.

Ramanan N, Shen Y, Sarsfield S, Lemberger T, Schutz G, Linden DJ, Ginty DD. 2005. SRF mediates activity-induced gene expression and synaptic plasticity but not neuronal viability. Nat Neurosci. 8:759-767.

Rammes G, Steckler T, Kresse A, Schutz G, Zieglgansberger W, Lutz B. 2000. Synaptic plasticity in the basolateral amygdala in transgenic mice expressing dominant-negative cAMP response element-binding protein (CREB) in forebrain. Eur J Neurosci. 12:2534-2546.

Riccio A, Ahn S, Davenport CM, Blendy JA, Ginty DD. 1999. Mediation by a CREB family transcription factor of NGF-dependent survival of sympathetic neurons. Science. 286:2358-2361.

Rostock A, Tober C, Rundfeldt C, Bartsch R, Engel J, Polymeropoulos EE, Kutscher B, Loscher W, Honack D, White HS, Wolf HH. 1996. D-23129: a new anticonvulsant with a broad spectrum activity in animal models of epileptic seizures. Epilepsy research. 23:211-223.

Shumyatsky GP, Tsvetkov E, Malleret G, Vronskaya S, Hatton M, Hampton L, Battey JF, Dulac C, Kandel ER, Bolshakov VY. 2002. Identification of a signaling network in lateral nucleus of amygdala important for inhibiting memory specifically related to learned fear. Cell. 111:905-918.

Storm JF. 1989. An after-hyperpolarization of medium duration in rat hippocampal pyramidal cells. J Physiol. 409:171-190.

Sugars KL, Brown R, Cook LJ, Swartz J, Rubinsztein DC. 2004. Decreased cAMP response element-mediated transcription: an early event in exon 1 and full-length cell models of Huntington's disease that contributes to polyglutamine pathogenesis. J Biol Chem. 279:4988-4999.

Tanis KQ, Duman RS, Newton SS. 2008. CREB binding and activity in brain: regional specificity and induction by electroconvulsive seizure. Biol Psychiatry. 63:710-720.

Tischmeyer W, Grimm R. 1999. Activation of immediate early genes and memory formation. Cell Mol Life Sci. 55:564-574.

Viosca J, Schuhmacher AJ, Guerra C, Barco A. 2008. Germ line expression of H-RasG12V causes neurological deficits associated to Costello syndrome. Genes Brain Behav. Sep 22 [Epub ahead of print].

Vitolo OV, Sant'Angelo A, Costanzo V, Battaglia F, Arancio O, Shelanski M. 2002. Amyloid beta -peptide inhibition of the PKA/CREB pathway and long-term potentiation: reversibility by drugs that enhance cAMP signaling. Proc Natl Acad Sci U S A. 99:13217-13221.

Wang HS, Pan Z, Shi W, Brown BS, Wymore RS, Cohen IS, Dixon JE, McKinnon D. 1998. KCNQ2 and KCNQ3 potassium channel subunits: molecular correlates of the M-channel. Science. 282:1890-1893.

Zhang X, Odom DT, Koo SH, Conkright MD, Canettieri G, Best J, Chen H, Jenner R, Herbolsheimer E, Jacobsen E, Kadam S, Ecker JR, Emerson B, Hogenesch JB, Unterman T, Young RA, Montminy M. 2005. Genome-wide analysis of cAMP-response element binding protein occupancy, phosphorylation, and target gene activation in human tissues. Proc Natl Acad Sci U S A. 102:4459-4464.

Zhu P, Aller MI, Baron U, Cambridge S, Bausen M, Herb J, Sawinski J, Cetin A, Osten P, Nelson ML, Kugler S, Seeburg PH, Sprengel R, Hasan MT. 2007. Silencing and un-silencing of tetracycline-controlled genes in neurons. PLoS ONE. 2:e533.

Figure Legends

Figure 1. Regulated expression of A-CREB in the brain of transgenic mice: A. Scheme presenting the inhibition of CREB-mediated gene expression achieved in our transgenic approach. **B.** *In situ* hybridization on brain sagittal sections from CaMKII-tTA/tetO-A-CREB-95 bitransgenic mice (A-CREB) and a wild-type littermate (WT) using an oligonucleotide probe specific for A-CREB. **C.** Transgene expression detected by DIG *in situ* hybridization with a probe specific for A-CREB transgene in 2-week old mice. **D.** Western-blot using anti-M2 Flag antibody detected A-CREB expression in hippocampal protein extracts. **E.** qRT-PCR quantification of CREB mRNA in the hippocampus of A-CREB (black bar) mice and control littermates (white bar) (3 mice per group, p=0.66). **F**. Immunostaining of brain sections of 14 days old A-CREB mice showed that CREB immunoreactivity was reduced in those areas with higher transgene expression, such as the CA1 subfield. **G.** DIG *in situ* hybridization showing repression of transgene expression in 5 weeks old A-CREB mice fed with dox food for 2 weeks (ON/OFF). Strong expression was detected in 3 weeks old mice maintained off dox (ON). **H.** DIG *in situ* hybridization showing defective transgene induction in A-CREB mice receiving dox during embryonic and postnatal development. No expression was detected in 8 weeks old mice maintained on dox (OFF). Transgene induction was assessed in 8 weeks old mice after having removed dox for four weeks (OFF/ON). Scale bar: 140 μm.

Figure 2. Neuronal loss in the hippocampus of A-CREB mice. **A.** A-CREB mice (◆, n=7) did not gain weight in the same progression that control littermates (□, n=18). **B.** Time course of the reduction of transgene expression detected by DIG *in situ* hybridization. Compare with the result obtained at 2 weeks (Fig. 1C, see also Supplementary Figure S1C). **C.** Nissl staining of the hippocampus of A-CREB mice

at different times after transgene induction. Hippocampus morphology in 3 weeks old A-CREB mice (A-CREB 3w) and control littermates are undistinguishable. However, seven weeks later (A-CREB 10w), massive loss of neurons was observed in the CA1 subfield. At least two mice were analyzed per time point. The age of onset of neurodegeneration was between 4 and 8 weeks. Severe cell loss was reliably detected in mice older than 10 weeks. Scale bar: 140 μm. **D.** We quantified the loss of neurons in different brain regions in adult A-CREB mice (≥6 months old; WT: n=6; A-CREB: n=7): CA1: The thickness of the CA1 cellular layer was significantly reduced in A-CREB mice ($p<0.001$). DG: The thickness of the dentate gyrus upper and lower blades was slightly reduced in A-CREB mice ($p<0.001$). Cortex: The thickness of the cortex was significantly reduced in A-CREB mice ($p<0.001$), but no change in cell density was observed ($p=0.14$). Layers 2 and 3, in which transgene expression is stronger (DIG in situ at the right panel and Fig. 1B), were particularly affected (layer 2/3: $p<0.001$; layer 5: $p=0.04$), but still showed transgene expression. **E.** Neuronal loss was prevented by feeding the mice with dox before the onset of cellular death (A-CREB 3w On/8w Off) and was triggered in adulthood by removing dox from the mouse diet (A-CREB 3w On/8w Off/3w On).

Figure 3. Impaired plasticity in the hippocampus of A-CREB mice. A. Input-output curve of fEPSP slope (V/s) versus stimulus (V) at the Schaffer collateral pathway of hippocampal slices from 3-week old A-CREB mice (●, n= 24) and control littermates (□, n=28) ($p=0.18$). **B.** Comparison of pair-pulse facilitation in 3-weeks old A-CREB mice and control littermates. Data are presented as the mean±SEM of the facilitation of the second response relative to the first response **C**. Cumulative probability versus area of the power spectra calculated from 250 s recordings at the CA1 pyramidal layer in hippocampal slices from 3-weeks old

control (n=29) and A-CREB mice (n=26, p=0.70). **D.** A single 100 Hz train (1 sec) evoked E-LTP in hippocampal slices of 3-weeks old control and A-CREB mice. **E.** Four 100 Hz trains evoked L-LTP was impaired in 3-weeks old A-CREB mice.

Figure 4. Neuronal excitability is reduced in CA1 neurons expressing A-CREB. **A.** Representative CA1 neuron response to 200 and 300 pA depolarizing pulses in a 3-weeks old control (left panel) and an A-CREB mouse (right panel). **B.** Average of APs triggered in response to increasing depolarizing currents in CA1 neurons from 3-weeks old A-CREB mice (●) and control littermates (□, upper panel $p<0.001$ ANOVA). This effect was reversed ten days after turning off A-CREB expression with dox (lower panel, $p=0.33$). **C.** Voltage-current relationship in CA1 pyramidal neurons holding at -70 mV in 3-weeks old A-CREB mice and control littermates. The alterations in A-CREB mice were reversed in the presence of the M-current blocker XE-991 (10 μM) (**D),** and after transgene repression by dox for ten days (**E**).

Figure 5. Seizure susceptibility in mice with enhanced or reduced CREB activity in neurons. A. Five-weeks old A-CREB mice (●) and control (□) littermates were intraperitoneally injected with 50 mg/Kg of PTZ every day until seizure stage 5 was consistently observed in both groups (n=6 for both groups). **B.** The same protocol was used in five-week old VP16-CREB^{high} mice (▲) and their littermates (□) (n=6 for both groups). The first PTZ injection was administered one week after transgene induction by dox removal. Note the stronger response to the drug in mutant mice observed already after the first injection. The average scaling is presented as mean ± SEM.

Figure 6. Gene expression analysis of early transcriptional changes in A-CREB mice. A. Three-weeks old A-CREB mice (n=7) showed milder seizures than their control littermates (n=10) in response to 14 mg/Kg of kainic acid. **B.** Two-

dimensional hierarchical clustering of 21 probe sets significantly affected by genotype in the two-way ANOVA analysis and showing at least 2 fold change in the comparison between genotypes in animals injected either with saline or kainate. The right panels show the clusters obtained by *K*-means clustering. 1: WTSAL, wild-type saline; 2: WTKA14, wild-type injected with 14 mg/Kg of kainate; 3: ACSAL, A-CREB saline; 4: ACKA14, A-CREB with 14 mg/Kg; and 5: ACKA18, A-CREB with 18 mg/Kg kainate (see also Supplementary Table 2). **C.** Results of hybridization for perfect match (PM) oligonucleotide probes in the probe set 1452529_a_at. The direct observation of the hybridization signals revealed a large increase in the signal corresponding to the only two oligonucleotides complementary to A-CREB sequence. **D.** Hieralchical clustering of the 209 probe sets significantly affected by drug treatment in the two-way ANOVA analysis showing a fold change equal or bigger than 2 in the comparison between drug treatments for at least one of the two genotypes. A number of genes in this list, specially those presenting largest changes (bright red traces in KA samples) have been previously identified as IEGs, including *arc*, *egr2*, *egr3*, *c-fos*, *fosB*, *crem* and *junB* (see Table 1 and Supplementary Table 3 for additional details). **E.** Whisker box representation of expression changes in the group of 209 probe sets showed in panel 6D. **F.** *In situ* hybridization using DIG-RNA probes specific for Arc (upper panels) and BDNF (lower panels) in sagittal brain sections of 3 weeks old A-CREB mice and control littermates injected with vehicle or with 14 or 18 mg/Kg of kainic acid. Correlating with seizure strength, some A-CREB mice injected with 14 mg/Kg of kainic acid showed very weak induction of IEGs (see example in central panels), whereas other mice showed an induction similar to that observed in control littermates or in A-CREB mice injected with 18 mg/Kg of kainic acid (right panels). Similar results were obtained by immunohistochemistry using

antibodies against c-Fos and Egr1 (results not shown). **G.** Quantitative RT-PCR of Arc and c-Fos levels in the hippocampus of 3-weeks old A-CREB mice and control siblings two hours after injection with 14 mg/Kg of kainate (KA). From left to right: WT saline (n=3): white bars; WT KA (n=3): light gray bars; A-CREB saline (n=3): black bars; A-CREB KA (n=3): dark gray bars. We observed a significant reduction in the basal level of Arc expression (p=0.04), but not for c-Fos (p=0.38). **H.** Quantitative RT-PCR of Arc and c-Fos levels in the hippocampus of 3-weeks old A-CREB and control siblings after exploration of a novel environment for 1 hour. From left to right: WT homecage (n=5): white bars; WT novelty (n=6): light gray bars; A-CREB homecage (n=5): black bars; A-CREB novelty (n=5): dark gray bars. There is a significant reduction in the basal level of Arc expression in A-CREB mice (p=0.04). **I.** CREM immunostaining of the hippocampus of a 3-weeks old A-CREB mouse did not reveal an increase in CREM immunoreactivity (3 mice per group). **J.** qRT-PCR quantification of CREM mRNA in the hippocampus of 3-weeks old A-CREB (black bar) mice and control littermates (white bar) (3 mice per group, p=0.69).

Figure 7. Long-term consequences of chronic inhibition of CREB function by A-CREB. A. Input/output curve of fEPSP slope (V/s) versus stimulus at the Schaffer collateral pathway of hippocampal slices from one year old A-CREB mice (●, n= 23) and control littermates (□, n=26, p=0.01). **B.** Ten-week old A-CREB mice (black) show hyperlocomotion (left panel, ambulatory distance during a 30 min period: wild type, n = 11; A-CREB; n=9; p=0.01) and a trend towards reduced anxiety behavior in an open field (right panel, percentage of time spent in the center of the arena, p=0.14). **C.** Spatial navigation in the Morris water maze in adult A-CREB mice (A-CREB: n=9; WT: n=11). Path length analysis revealed deficits associated with chronic A-CREB expression in both the visible platform and the hidden platform tasks (ANOVA

repeated measures, genotype effect: visible platform, p=0.09; hidden platform, p=0.01). Similar deficits were also observed in escape latencies (ANOVA repeated measures, genotype effect: visible platform, p=0.01; hidden platform, p=0.001). Swimming speed and thigmotaxis were not significantly affected. **D** Spatial memory was assessed in two probe trials. Values represent percentage of time in the target quadrant compared to the average in other quadrants (grey bars). Control mice spent more time in the platform quadrant in the two probe trials, whereas A-CREB mice did not show a memory for the platform location (chance value: 25%). Asterisks indicate $p<0.05$.

Table 1. The induction of immediate early genes related to synaptic plasticity is largely unimpaired in A-CREB mice. See full list of activity-driven genes in Supplemental Table 3

Gene	Probe Set ID	Gene Title	Unigene ID	FC-WT	FC-AC KA14	FC-AC KA18	*P*	CRE
Arc	1418687_at	activity regulated cytoskeletal-associated protein	Mm.25405	3.57	6.41	5.75	0.002	2
Atf3	1449363_at	activating transcription factor 3	Mm.2706	13.24	13.50	9.80	>0.001	3
Bdnf	1422169_a_at	brain derived neurotrophic factor	Mm.1442	3.30	3.43	2.37	>0.001	1
	1422168_a_at			4.50	4.57	3.59	>0.001	
Btg2	1448272_at	B-cell translocation gene 2	Mm.392646	4.27	4.93	6.03	>0.001	5
	1416250_at			8.59	7.39	9.07	>0.001	
Crem	1449037_at	cAMP responsive element modulator	Mm.5244	1.91	2.35	2.31	0.006	1
	1418322_at			2.33	3.51	3.02	0.002	
Dusp1	1448830_at	dual specificity phosphatase 1	Mm.239041	3.18	4.31	4.77	>0.001	2
Dusp4	1428834_at	dual specificity phosphatase 1	Mm.392187	2.69	2.75	1.88	0.003	6
Egr1	1417065_at	early growth response 1	Mm.181959	1.84	3.27	3.10	0.001	5
Egr2	1427682_a_at	early growth response 2	Mm.290421	5.35	12.95	12.95	>0.001	3
	1427683_at			5.60	14.70	12.50	>0.001	
Egr3	1436329_at	early growth response 3	Mm.103737	2.18	3.16	2.50	0.006	5
Egr4	1449977_at	early growth response 4	Mm.44137	3.99	4.64	3.64	>0.001	4
Fos	1423100_at	FBJ osteosarcoma oncogene	Mm.246513	9.57	12.74	12.09	>0.001	9
Fosb	1422134_at	FBJ osteosarcoma oncogene B	Mm.248335	15.37	24.59	19.02	>0.001	7
Fosl2	1422931_at	fos-like antigen 2	Mm.24684	1.67	2.27	2.16	0.005	5
	1437247_at			2.47	5.08	3.63	>0.001	
Gadd45b	1449773_s_at	growth arrest and DNA-damage-inducible 45 beta	Mm.1360	5.70	7.28	5.57	>0.001	3
	1450971_at			5.85	6.30	4.57	>0.001	
Homer1	1425671_at	homer homolog 1 (Drosophila)	Mm.37533	8.82	10.34	6.15	0.002	4
Ier2	1416442_at	immediate early response 2 (Etr101)	Mm.399	4.05	5.68	6.31	0.002	4
Jun	1448694_at	Jun oncogene	Mm.275071	1.60	2.12	2.03	0.001	4
	1417409_at			2.43	2.60	2.50	0.002	
Junb	1415899_at	Jun-B oncogene	Mm.1167	4.79	5.39	4.63	>0.001	6
Klf4	1417394_at	Kruppel-like factor 4 (gut)	Mm.4325	2.50	4.58	3.94	0.001	2
	1417395_at			3.00	5.40	5.02	>0.001	
Npas4	1459372_at	Neuronal PAS domain protein 4	Mm.287867	41.91	64.60	53.89	>0.001	5
Nr4a1	1416505_at	nuclear receptor subfamily 4, group A, member 1 (Nur77)	Mm.119	3.05	3.93	3.81	0.001	6
Nr4a2	1450749_a_at	nuclear receptor subfamily 4, group A, member 1 (Nurr-1)	Mm.3507	2.91	2.97	2.17	0.002	6
	1455034_at			2.98	3.52	2.82	>0.001	
	1450750_a_at			3.05	3.88	3.13	0.001	
	1447863_s_at			3.43	3.81	2.88	0.001	
Pim1	1435458_at	proviral integration site 1	Mm.328931	2.90	3.01	2.07	>0.001	4
	1435872_at			5.03	5.96	4.61	>0.001	
Rgs2	1419248_at	regulator of G-protein signaling 2	Mm.28262	3.68	4.90	4.27	>0.001	4
	1447830_s_at			3.98	5.58	4.82	>0.001	
	1419247_at			4.74	6.11	5.25	>0.001	
Slc2a1	1426599_a_at	solute carrier family 2 member 1 (Glut-1)	Mm.21002	1.60	2.04	1.61	0.003	1

FC WT = fold change wild-type saline vs. wild-type 14 mg/Kg kainate; FC AC KA14 = fold change A-CREB saline vs. A-CREB 14 mg/Kg kainate; FC AC KA18 = fold change A-CREB saline vs. A-CREB 18 mg/Kg kainate. CRE = number of CRE predicted in murine promoters (3 Kb upstream and 200 bp downstream of the transcription start site, see Zhang et al. (2005), *PNAS* 102:4459-64, for further details). P values correspond to two-way ANOVA described in Supplementary Methods. Note that as a consequence of reduced basal expression, the fold change of some IEGs (*arc*, *egr1*, *egr2*) was larger in A-CREB mice (see also Supplementary Table 4).

Table 2. Probe sets targeted to members of the CREB family of transcription factors

Probe Set ID	FC	p-value	Unigene ID	Gene Symbol	Gene Description
1417296_at	1.03	0.80	Mm.676	*Atf1*	activating transcription factor 1
1421582_a_at	1.00	0.99	Mm.466618	*Creb1*	cAMP responsive element binding protein 1
1423402_at	1.50	0.27			
1452529_a_at [1]	1.39	0.60			
1428755_at	1.16	0.42			
1452901_at	1.09	0.48			
1418322_at [2]	-1.00	1.00	Mm.5244	*Crem*	cAMP responsive element modulator
1449037_at [2]	1.19	0.65			
1430847_a_at	1.15	0.38			

FC = fold change wild-type saline vs. A-CREB saline. P values correspond to unpaired t-Test analysis.
[1] Probe set 1452529_a_at contains two probes that recognize a sequence common to A-CREB and wild type CREB (Figure 6C). This abnormal pattern of upregulation, affecting only two probes out of 11 escaped conventional screening using GCOS and GeneSpring, but dChip revealed a fold change > 10 (the largest change between wild type and A-CREB mice), when no correction for outlier probes was considered.
[2] Probe sets 1418322_at and 1449037_at are targeted to the 3'UTR of CREM and can recognize the transcripts encoding the inducible repressor isoform ICER. The signals for both probe sets were not affected by transgene expression, but significantly increased in kainate treated samples (see Table 1). Probe set 1430847_a_at, which is targeted to the 2nd Q-rich domain specific of CREMτ, showed changes neither by kainate nor by transgene expression.

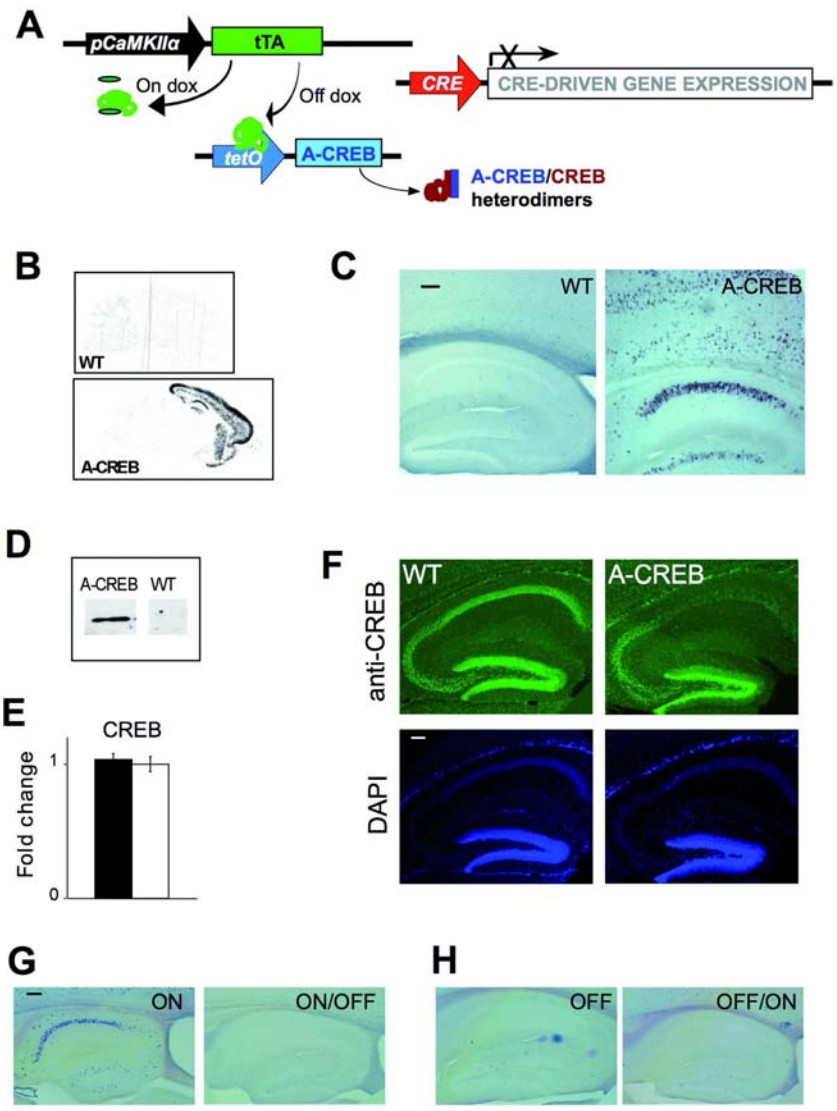

180x242mm (300 x 300 DPI)

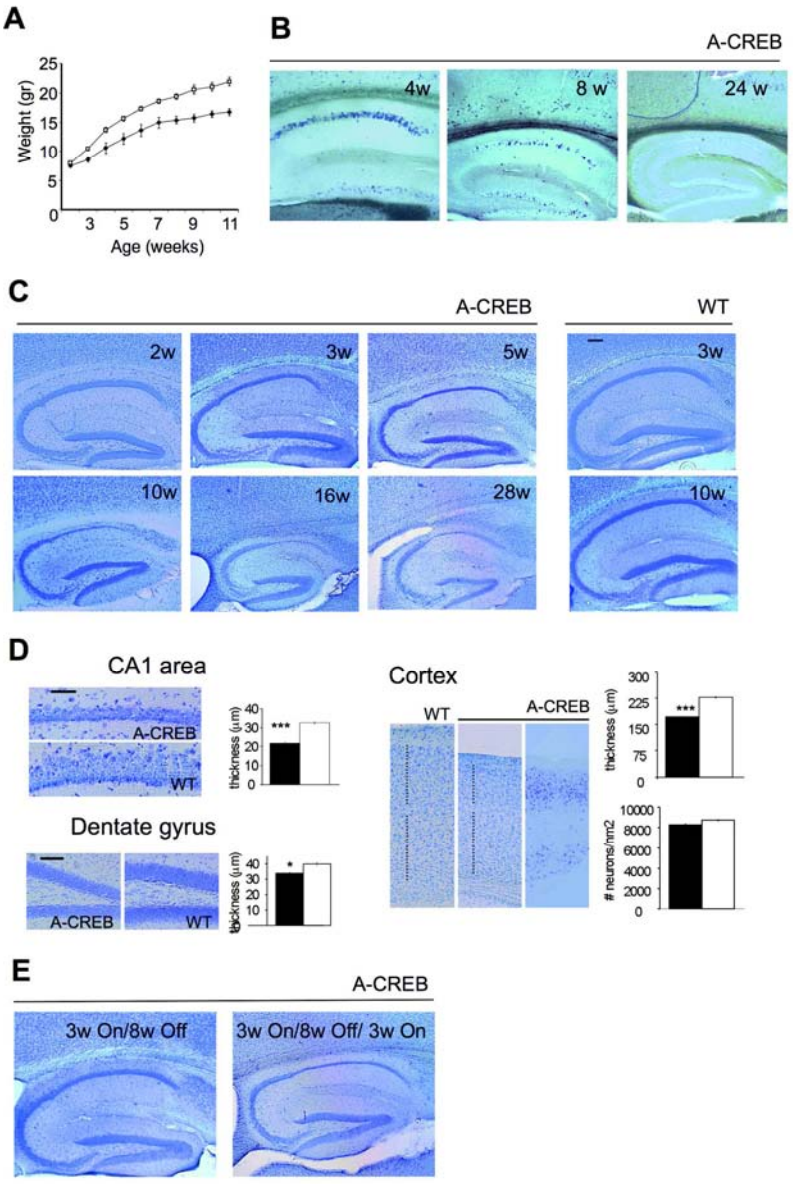

180x265mm (300 x 300 DPI)

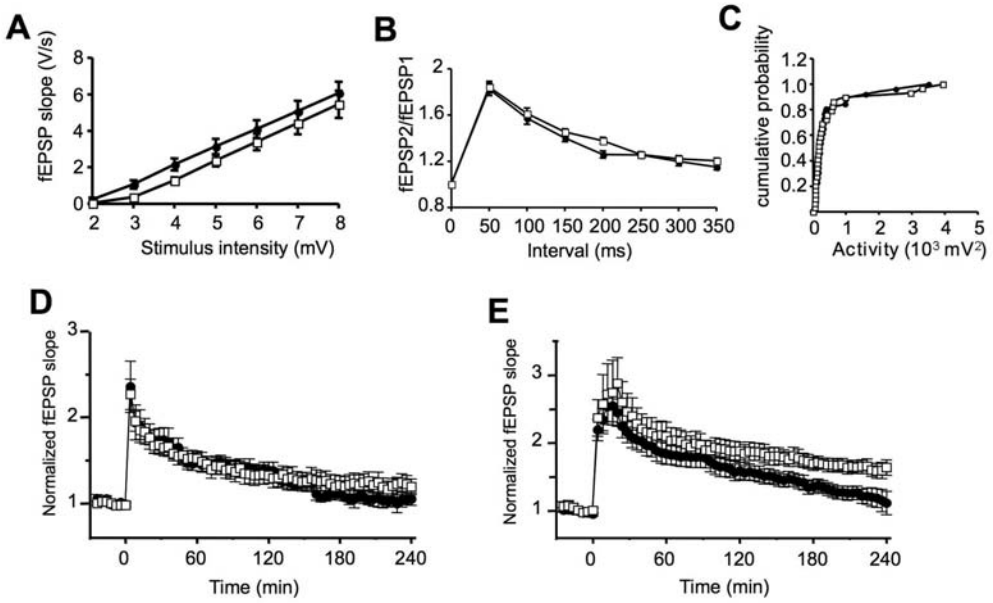

180x113mm (600 x 600 DPI)

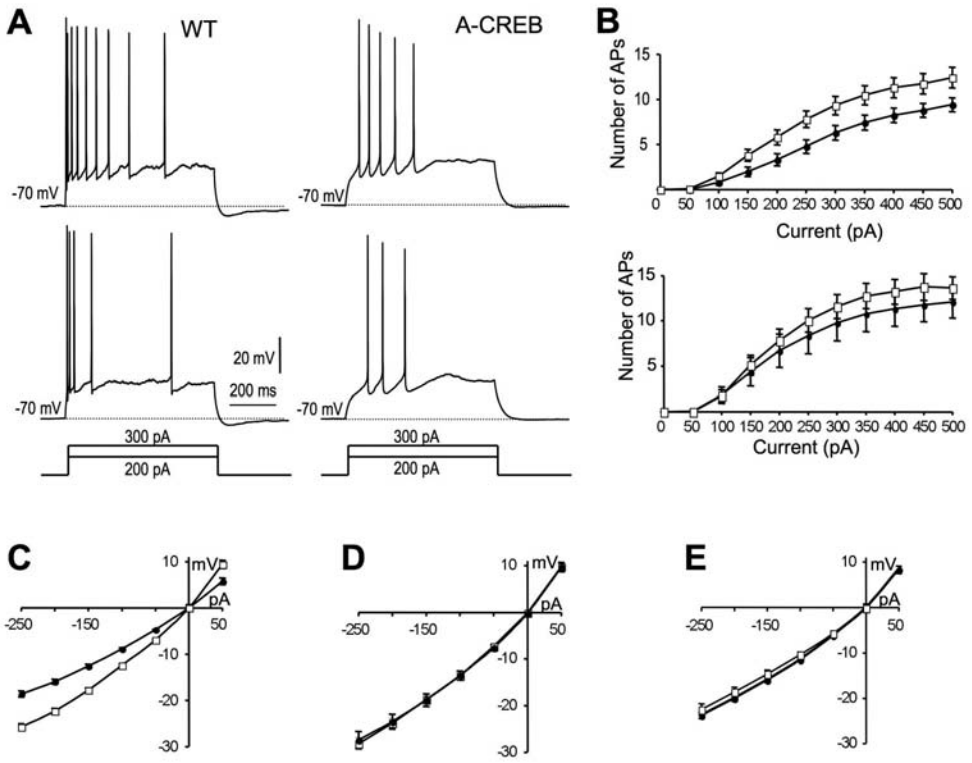

180x144mm (600 x 600 DPI)

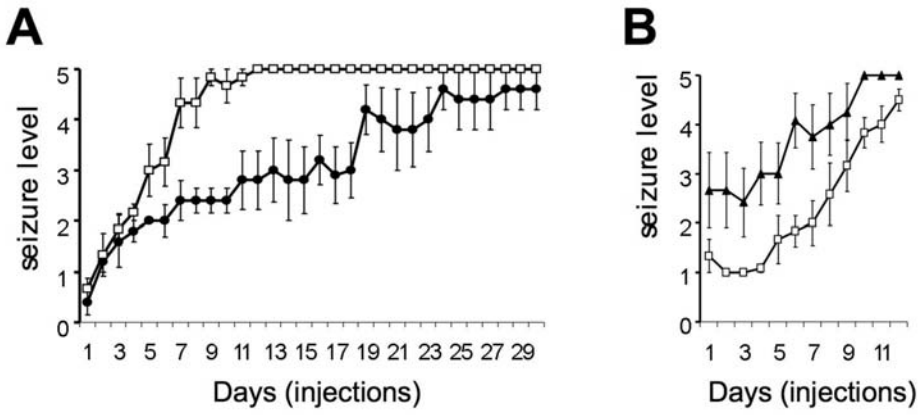

180x89mm (600 x 600 DPI)

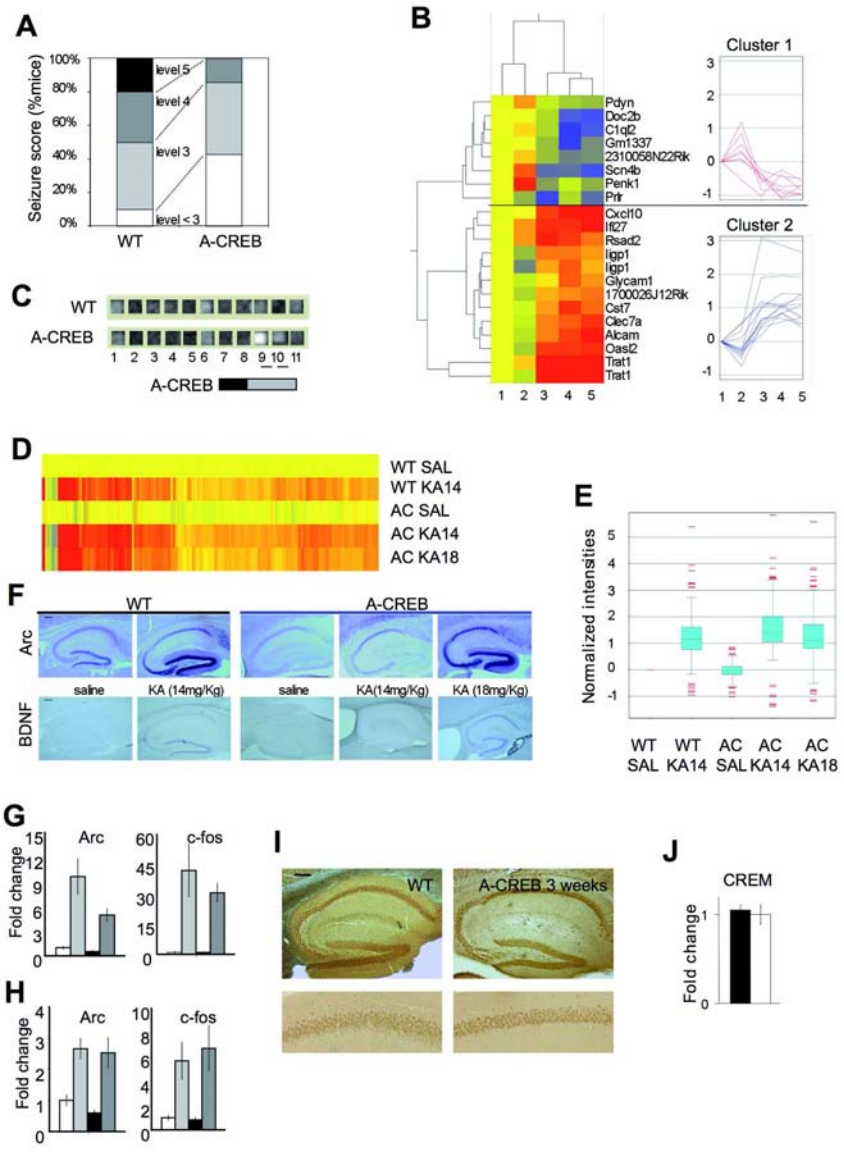

180x240mm (300 x 300 DPI)

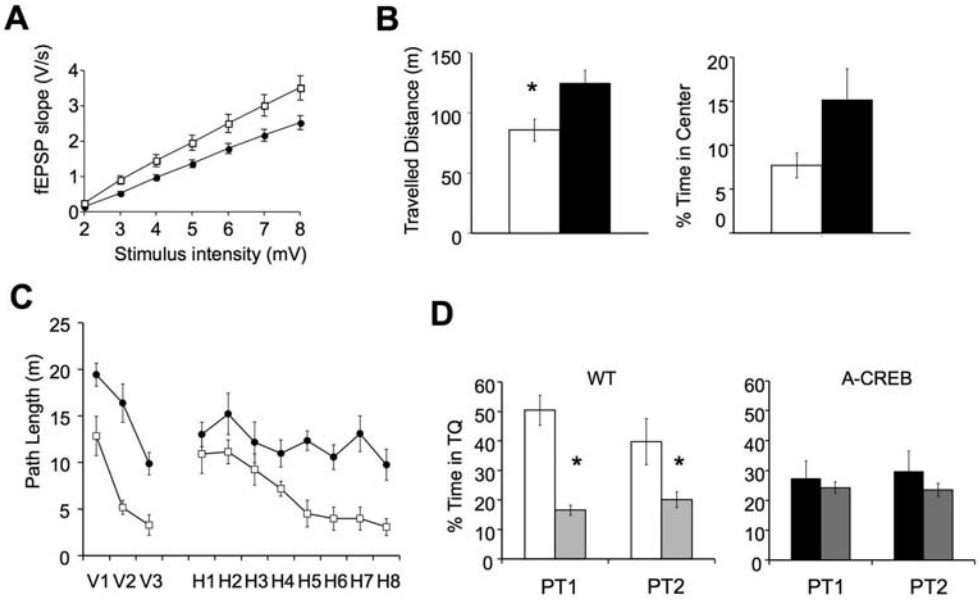

180x114mm (600 x 600 DPI)

SUPPLEMENTARY MATERIAL

Supplementary Methods

Microarray analysis

Each sample contained total RNA from the hippocampi of a group of 3-4 three weeks old mice. We obtained duplicate samples for each experimental condition (in total 14 WT and 20 A-CREB mice where used in this experiment). Mouse Genome 430 2.0 genechips were hybridized, stained, washed and screened for quality according to the manufacturer's protocol. The Affymetrix GeneChip® data were processed, normalized and statistically analyzed using GCOS (Affymetrix), GeneSpring GX (Agilent Technologies) and dChip softwares (Li & Hung Wong, 2001). After the normalization by the median intensities of the control arrays (WT saline), linearity of the signal intensities between arrays was confirmed and Principal Component Analysis (PCA) was performed to check the similarities of the arrays. GeneSpring and dChip softwares were used in parallel and produced highly overlapping lists of significantly changed probe sets. The lists presented in Supplemental Tables 2-4 were generated primarily using GeneSpring software because it permitted additional graphical representations and further statistical analyses, such as the *k*-means and hierarchical clustering (squared euclidean) showed in Figure 6. We considered two parameters in our analysis: genotype (wild-type or A-CREB) and drug (three conditions, saline, kainate 14 mg/Kg and kainate 18 mg/Kg). Given this experimental design, a two-way ANOVA was performed after filtering the data by expression level (signal intensities >20% of the maximal expression at least in two samples). We found 2000 genes significantly affected by drug treatment, 816 genes significantly affected by genotype and 426 in the genotype-drug interaction group (See Supplementary Tables 2-3 for full lists of probe sets showing a fold change equal or higher than 2 in relevant

comparisons). We also conducted a complementary pair-wise comparison analysis in GCOS to retrieve additional genes in the non-stimulated condition (wild-type saline vs. A-CREB saline). Probe sets retrieved in both pair-wise comparison replicates were compared to the list generated in the GeneSpring analysis to produce Supplemental Table 4.

Supplementary Tables

Supplementary Table 1. Electrophysiological properties of CA1 pyramidal neurons in A-CREB mice.

Supplementary Table 2. Genes altered in the hippocampus of A-CREB mice (GENOTYPE significant genes).

Supplementary Table 3. Genes altered in the hippocampus of A-CREB mice and control littermates after kainate treatment (DRUG significant genes).

Supplementary Table 4. Kainate-induced genes altered in the hippocampus of A-CREB mice at the basal state (Pair-wise significant genes).

Supplementary Table 5. Basal behavior analysis of A-CREB mice.

Supplementary Figures

Supplementary Figure S1. Pattern of transgene expression in line AC95. **A**. DIG *in situ* hybridization (ISH) with a probe specific for A-CREB transgene in brain sagittal sections from a 2-week old CaMKII-tTA/tetO-A-CREB-95 bitransgenic mouse (A-CREB). The lower panels show higher magnification images of striatum (left) and hippocampus and cortex (right). **B**. Transgene expression can also be detected by immunohistochemistry (IHC) using an antibody that recognizes the M2-Flag sequence in the N-terminus of A-CREB (red). As expected, the pattern of transgene expression using IHC and ISH was the same. **C**. Details of DIG-ISH using

a probe specific for A-CREB. Note the dramatic reduction of transgene expression in 16-week old A-CREB mice when compared to 2-week old mice.

Supplementary Figure S2. Immunohistochemical analysis of the hippocampus of A-CREB mice. The neurodegenerative process was also visualized by immunostaining with a number of neuronal markers. Floating vibratome sections (50 μM) were stained with antibodies against MAP2, GAP43, calbindin and synaptophysin. No significant differences were found in either hippocampus or other brain regions at early times (2 weeks old mice), but significant neuronal loss was observed after sustained CREB inhibition (28 weeks old mice).

Supplementary Table 1. Electrophysiological properties of CA1 pyramidal neurons in A-CREB mice

Group of mice (n=neurons, mice)	R_{in} (MΩ)	Rehobase (pA)	Medium I_{AHP} (pA)	slow I_{AHP} (pA)
A-CREB On (n=42, 6)	131±9.6	179±9.7	291±13.7	50±5.3
Control On (n=40, 5)	182±19.5	136±8.1	234±12.8	42±4.7
P	***0.01***	***0.001***	***0.003***	*0.26*
A-CREB On/Off (n=32, 4)	151±8.1	142±9.7	200±11.9	27±3.4
Control On/Off (n=17, 2)	159±23.7	144±15.2	143±12.1	31±6.1
P	*0.67*	*0.9*	***0.003***	*0.56*
A-CREB XE 991 (n=14, 3)	256±42	117±16.8	170±19.0	33±6.3
Control XE 991 (n=14, 2)	229±20	121±15.1	131±14.2	21±3.7
P	*0.56*	*0.87*	*0.11*	*0.11*

In A-CREB On mice and control littermates, the recordings were performed in 3-week old animals. In A-CREB On/Off mice and control littermates, the transgene was expressed for 3 weeks and then silenced for 10 additional days. Recording in neurons treated with XE 991 were performed in 3-week old mice.

Supplementary Table 2

Genes altered in the hippocampus of A-CREB mice (GENOTYPE significant genes, p<0,05)

Two-way ANOVA analysis: 21 genes out of 830 genes significantly affected by genotype exhibited a fold change larger than 2 in the comparison between genotypes in animals injected either with saline or kainate

Some genes, such as Scn4b and Penk1, are reduced both in animals injected with saline and kainate, whereas the genotype effect in other genes, such as Pdyn and Doc2b, is only evidenced in response to kainate

FC saline = fold change wild-type saline vs. A-CREB saline

FC KA14 = fold change wild-type 14 mg/Kg kainate vs. A-CREB 14 mg/Kg kainate

FC KA18 = fold change wild-type 14 mg/Kg kainate vs. A-CREB 18 mg/Kg kainate

CRE sites = number of CRE predicted in murine promoters (3 Kb upstream and 200 bp dowstream of the transcription start site, see Zhang et al. (2005), PNAS 102:4459-64, for further details)

n.d. = not determined / not found

Fold changes < 1.5 are indicated in gray

Genes downregulated in A-CREB mice

Probe Set ID	Gene Symbol	Gene Title	Unigene ID	FC saline	FC KA14	FC KA18	P value	CRE sites
1437397_at	Prlr	prolactin receptor	Mm.442298	-2,04	1,12	-1,24	0,0331	4
1434008_at	Scn4b	sodium channel, type IV, beta	Mm.335112	-1,80	-3,21	-3,52	0,0357	n.d.
1427038_at	Penk1	preproenkephalin 1	Mm.2899	-1,54	-2,69	-3,33	0,0268	n.d.
1443287_at	Gm1337	gene model 1337, (NCBI)	Mm.35758	-1,42	-2,22	-1,73	0,0057	n.d.
1429215_at	2310058N22Rik	RIKEN cDNA 2310058N22 gene	Mm.440654	-1,40	-2,10	-2,03	0,0066	n.d.
1444687_at	C1ql2	complement component 1, q subcomponent-like 2	Mm.337409	-1,30	-2,55	-2,31	0,0029	n.d.
1420666_at	Doc2b	double C2, beta	Mm.5137	-1,29	-1,98	-2,04	0,0225	n.d.
1416266_at	Pdyn	prodynorphin	Mm.6239	-1,20	-1,94	-2,02	0,0108	2

Genes upregulated in A-CREB mice

Probe Set ID	Gene Symbol	Gene Title	Unigene ID	FC saline	FC KA14	FC KA18	P value	CRE sites
1427532_at	Trat1	T cell receptor associated transmembrane adaptor 1	Mm.167298	8,47	5,87	5,11	1,0E-05	n.d.
1437561_at	Trat1	T cell receptor associated transmembrane adaptor 1	Mm.167298	3,72	4,76	4,61	1,7E-05	n.d.
1421009_at	Rsad2	radical S-adenosyl methionine domain containing 2	Mm.24045	2,28	1,42	1,12	0,0450	n.d.
1426278_at	Ifi27	interferon, alpha-inducible protein 27	Mm.271275	2,16	1,47	1,66	0,0315	n.d.
1453196_a_at	Oasl2	2'-5' oligoadenylate synthetase-like 2	Mm.228363	2,05	2,76	2,90	0,0017	2
1418930_at	Cxcl10 /// LOC100045000	chemokine (C-X-C motif) ligand 10	Mm.877	2,00	2,50	2,47	0,0030	4
1419042_at	Iigp1 /// LOC100044196	interferon inducible GTPase 1	Mm.261140	1,63	2,29	2,02	0,0202	1
1420699_at	Clec7a	C-type lectin domain family 7, member a	Mm.239516	1,54	2,10	2,50	0,0047	n.d.
1443086_at	Alcam	activated leukocyte cell adhesion molecule	Mm.288282	1,54	2,52	3,33	0,0142	4
1419202_at	Cst7	cystatin F (leukocystatin)	Mm.12965	1,42	2,43	1,91	0,0288	0
1419043_a_at	Iigp1 /// LOC100044196	interferon inducible GTPase 1	Mm.261140	1,39	2,99	2,20	0,0029	1
1453793_at	1700026J12Rik	RIKEN cDNA 1700026J12 gene	Mm.307720	1,33	1,96	2,14	0,0299	n.d.
1424825_a_at	Glycam1	glycosylation dependent cell adhesion molecule 1	Mm.219621	1,14	2,14	1,73	0,0419	0

Supplementary Table 3

Genes altered in the hippocampus of A-CREB mice and control littermates after kainate treatment (DRUG significant genes, p>0.05)

Two-way ANOVA analysis: 209 genes out of 2025 genes significantly affected by drug treatment exhibited a fold change larger than 2 in the comparison between drug treatments in animals of either genotype

FC WT = fold change wild-type saline vs. wild-type 14 mg/Kg kainate

FC AC KA14 = fold change A-CREB saline vs. A-CREB 14 mg/Kg kainate

FC AC KA18 = fold change A-CREB saline vs. A-CREB 18 mg/Kg kainate

CRE sites = number of CRE predicted in murine promoters (3 Kb upstream and 200 bp dowstream of the transcription start site, see Zhang et al. (2005), PNAS 102:4459-64, for further details)

n.d. = not determined

Fold changes < 2 are indicated in grey

Probe Set ID	Gene Symbol	Gene Title	Unigene ID	FC saline	FC KA14	FC KA18	P value	CRE sites
1459372_at	Npas4	neuronal PAS domain protein 4	Mm.287867	41,91	64,60	53,89	2,1E-06	5
1422134_at	Fosb	FBJ osteosarcoma oncogene B	Mm.248335	15,37	24,59	19,02	3,0E-05	7
1449363_at	Atf3	activating transcription factor 3	Mm.2706	13,24	13,50	9,80	3,0E-05	3
1417262_at	Ptgs2	prostaglandin-endoperoxide synthase 2	Mm.292547	9,68	11,17	8,62	2,4E-05	2
1423100_at	Fos	FBJ osteosarcoma oncogene	Mm.246513	9,57	12,74	12,09	2,8E-06	9
1417263_at	Ptgs2	prostaglandin-endoperoxide synthase 2	Mm.292547	9,42	10,58	8,84	3,1E-05	2
1425671_at	Homer1	homer homolog 1 (Drosophila)	Mm.37533	8,82	10,34	6,15	0,0018	4
1416250_at	Btg2	B-cell translocation gene 2, anti-proliferative	Mm.392646	8,59	7,39	9,07	4,2E-04	5
1450842_a_at	Cenpa	centromere protein A	Mm.290563	8,55	6,51	3,81	4,7E-05	3
1422053_at	Inhba	inhibin beta-A	Mm.8042	6,60	8,90	7,45	7,1E-05	3
1450971_at	Gadd45b	growth arrest and DNA-damage-inducible 45 beta	Mm.1360	5,85	6,30	4,57	1,9E-04	3
1449773_s_at	Gadd45b	growth arrest and DNA-damage-inducible 45 beta	Mm.1360	5,70	7,28	5,57	5,7E-05	3
1438133_a_at	Cyr61	cysteine rich protein 61	Mm.1231	5,68	11,19	11,44	1,5E-04	8
1427683_at	Egr2	early growth response 2	Mm.290421	5,60	14,70	12,50	3,7E-05	3
1427682_a_at	Egr2	early growth response 2	Mm.290421	5,35	12,95	12,95	1,8E-04	3
1426063_a_at	Gem	GTP binding protein (gene overexpressed in skeletal muscle)	Mm.247486	5,25	9,99	8,18	3,3E-04	5
1453851_a_at	Gadd45g	growth arrest and DNA-damage-inducible 45 gamma	Mm.281298	5,05	7,65	8,72	1,7E-04	3
1435872_at	Pim1	Proviral integration 1	Mm.472907	5,03	5,96	4,61	1,1E-05	4
1417483_at	Nfkbiz	nuclear factor of kappa light polypeptide gene enhancer in B-cells inhibitor, zeta	Mm.247272	4,85	6,55	4,90	1,2E-04	n.d.
1415899_at	Junb	Jun-B oncogene	Mm.1167	4,79	5,39	4,63	6,7E-04	6
1419816_s_at	Errfi1	ERBB receptor feedback inhibitor 1	Mm.318841	4,78	4,62	3,84	4,1E-04	n.d.
1421811_at	LOC640441 /// Thbs1	thrombospondin 1 /// similar to thrombospondin 1	Mm.4159	4,78	6,97	4,08	2,7E-04	1
1419247_at	Rgs2	regulator of G-protein signaling 2	Mm.28262	4,74	6,11	5,25	5,0E-05	4
1429444_at	Rasl11a	RAS-like, family 11, member A	Mm.266978	4,72	3,76	3,03	2,3E-04	n.d.
1422168_a_at	Bdnf	brain derived neurotrophic factor	Mm.1442	4,50	4,57	3,59	2,3E-04	1
1416129_at	Errfi1	ERBB receptor feedback inhibitor 1	Mm.318841	4,42	5,03	4,27	4,7E-05	n.d.
1436387_at	C330006P03Rik	RIKEN cDNA C330006P03 gene		4,29	10,25	6,95	8,7E-04	n.d.
1448272_at	Btg2	B-cell translocation gene 2, anti-proliferative	Mm.392646	4,27	4,93	6,03	2,8E-04	5
1418250_at	Arl4d /// LOC100044157	ADP-ribosylation factor-like 4D /// hypothetical protein LOC100044157	Mm.266840	4,21	4,81	4,69	0,0012	n.d.
1416039_x_at	Cyr61	cysteine rich protein 61	Mm.1231	4,14	10,46	11,47	1,4E-04	8
1416442_at	Ier2	immediate early response 2	Mm.399	4,05	5,68	6,31	0,0018	4
1420720_at	LOC100044234 /// Nptx2	neuronal pentraxin 2 /// hypothetical protein LOC100044234	Mm.10099	4,01	4,78	3,07	0,0061	3
1449977_at	Egr4	early growth response 4	Mm.44137	3,99	4,64	3,64	1,3E-04	4
1447830_s_at	Rgs2	regulator of G-protein signaling 2	Mm.28262	3,98	5,58	4,82	6,7E-05	4
1449960_at	Nptx2	neuronal pentraxin 2	Mm.10099	3,83	4,86	3,45	1,2E-04	3
1452160_at	Tiparp	TCDD-inducible poly(ADP-ribose) polymerase	Mm.246398	3,76	4,63	4,09	3,3E-04	n.d.
1419248_at	Rgs2	regulator of G-protein signaling 2	Mm.28262	3,68	4,90	4,27	6,6E-05	4

1437884_at	Arl5b	ADP-ribosylation factor-like 5B	Mm.174068	3,67	4,73	3,26	0,0015	n.d.
1418687_at	Arc	activity regulated cytoskeletal-associated protein	Mm.25405	3,57	6,41	5,75	0,0025	2
1418932_at	LOC100046232 /// Nfil3	nuclear factor, interleukin 3, regulated / similar to NFIL3/E4BP4 transcription factor	Mm.136604	3,45	4,11	2,93	0,0027	6
1452161_at	Tiparp	TCDD-inducible poly(ADP-ribose) polymerase	Mm.246398	3,45	3,77	3,40	0,0015	n.d.
1416067_at	Ifrd1	interferon-related developmental regulator 1	Mm.168	3,43	4,97	4,30	6,5E-05	5
1447863_s_at	Nr4a2	nuclear receptor subfamily 4, group A, member 2	Mm.3507	3,43	3,81	2,88	0,0013	6
1455899_x_at	Socs3	suppressor of cytokine signaling 3	Mm.3468	3,35	6,37	4,25	1,9E-04	2
1455085_at	1700086L19Rik	RIKEN cDNA 1700086L19 gene	Mm.287421	3,32	2,58	2,44	3,2E-04	n.d.
1422169_a_at	Bdnf	brain derived neurotrophic factor	Mm.1442	3,30	3,43	2,37	8,0E-04	1
1427747_a_at	Lcn2	lipocalin 2	Mm.9537	3,22	2,63	1,65	0,0038	1
1455166_at	Arl5b	ADP-ribosylation factor-like 5B	Mm.174068	3,22	4,23	3,13	3,1E-04	n.d.
1448830_at	Dusp1	dual specificity phosphatase 1	Mm.239041	3,18	4,31	4,77	3,1E-04	2
1423294_at	Mest	mesoderm specific transcript	Mm.335639	3,12	4,47	3,41	8,5E-05	1
1448285_at	Rgs4	regulator of G-protein signaling 4	Mm.41642	3,07	3,47	3,02	4,2E-04	3
1416505_at	Nr4a1	nuclear receptor subfamily 4, group A, member 1	Mm.119	3,05	3,93	3,81	0,0010	6
1450750_a_at	Nr4a2	nuclear receptor subfamily 4, group A, member 2	Mm.3507	3,05	3,88	3,13	0,0012	6
1417051_at	Pcdh8	protocadherin 8	Mm.390715	3,05	2,76	2,25	7,2E-04	3
1455271_at	LOC620695	hypothetical protein LOC620695		3,05	2,68	2,47	0,0018	n.d.
1417394_at	Klf4	Kruppel-like factor 4 (gut)	Mm.473692	3,00	5,40	5,02	8,1E-04	2
1447825_x_at	Pcdh8	protocadherin 8	Mm.390715	2,99	3,18	2,74	7,6E-04	3
1455034_at	Nr4a2	nuclear receptor subfamily 4, group A, member 2	Mm.3507	2,98	3,52	2,82	3,6E-04	6
1450749_a_at	Nr4a2	nuclear receptor subfamily 4, group A, member 2	Mm.3507	2,91	2,97	2,17	0,0022	6
1435458_at	Pim1	proviral integration site 1	Mm.328931	2,90	3,01	2,07	1,7E-04	4
1418666_at	Ptx3	pentraxin related gene	Mm.276776	2,88	1,83	1,29	0,0063	1
1441228_at	Apold1	apolipoprotein L domain containing 1	Mm.296104	2,82	4,65	4,16	7,1E-05	n.d.
1444681_at	Erc2	ELKS/RAB6-interacting/CAST family member 2	Mm.318004	2,74	2,45	1,70	0,0020	n.d.
1427540_at	Zwint	ZW10 interactor	Mm.62876	2,73	3,92	2,89	0,0036	3
1429863_at	Lonrf3	LON peptidase N-terminal domain and ring finger 3	Mm.327654	2,73	2,34	1,81	8,2E-04	n.d.
1418936_at	Maff	v-maf musculoaponeurotic fibrosarcoma oncogene family, protein F (avian)	Mm.86646	2,70	4,21	2,89	2,0E-04	3
1428834_at	Dusp4	dual specificity phosphatase 4	Mm.170276	2,69	2,75	1,88	0,0026	6
1417406_at	Sertad1	SERTA domain containing 1	Mm.153684	2,67	3,06	2,19	0,0028	n.d.
1438796_at	Nr4a3	nuclear receptor subfamily 4, group A, member 3	Mm.247261	2,64	3,24	2,62	1,8E-04	2
1426870_at	Fbxo33	F-box protein 33	Mm.311026	2,63	3,16	2,79	1,8E-04	n.d.
1426721_s_at	Tiparp	TCDD-inducible poly(ADP-ribose) polymerase	Mm.246398	2,57	3,86	3,68	3,0E-04	n.d.
1456212_x_at	Socs3	suppressor of cytokine signaling 3	Mm.3468	2,57	4,48	3,12	1,7E-04	2
1437696_at	BC049807	cDNA sequence BC049807	Mm.441097	2,56	2,73	2,41	0,0064	n.d.
1436305_at	Rnf217	ring finger protein 217	Mm.295212	2,54	2,47	1,68	0,0025	n.d.
1426871_at	Fbxo33	F-box protein 33	Mm.311026	2,53	3,57	2,98	6,2E-04	n.d.
1460302_at	Thbs1	thrombospondin 1	Mm.4159	2,53	2,92	2,34	3,2E-04	1
1440179_x_at	Rnf217	ring finger protein 217	Mm.295212	2,52	2,70	1,91	0,0018	n.d.
1452352_at	Ctla2b	cytotoxic T lymphocyte-associated protein 2 beta	Mm.439734	2,51	3,55	2,27	0,0054	n.d.
1451280_at	Arpp21	cyclic AMP-regulated phosphoprotein, 21	Mm.297444	2,50	2,54	2,32	0,0121	n.d.
1417395_at	Klf4	Kruppel-like factor 4 (gut)	Mm.473692	2,50	4,58	3,94	0,0010	2
1434350_at	Axud1	AXIN1 up-regulated 1	Mm.125196	2,48	2,44	1,99	0,0001	7
1437247_at	Fosl2 /// LOC634417	fos-like antigen 2 /// similar to fos-like antigen 2	Mm.24684	2,47	5,08	3,63	5,5E-04	5
1453590_at	Arl5b	ADP-ribosylation factor-like 5B	Mm.174068	2,47	3,93	2,82	0,0012	n.d.
1416756_at	Dnajb1	DnaJ (Hsp40) homolog, subfamily B, member 1	Mm.282092	2,46	2,82	2,64	0,0030	6
1459941_at	Rlbp1l1	retinaldehyde binding protein 1-like 1	Mm.471888	2,45	2,50	1,52	0,0036	n.d.
1417409_at	Jun	Jun oncogene	Mm.275071	2,43	2,60	2,50	0,0017	4
1416811_s_at	Ctla2a /// Ctla2b	cytotoxic T lymphocyte-associated protein 2 alpha / cytotoxic T lymphocyte-associated protein 2 beta	Mm.439734	2,42	2,32	1,58	0,0114	3 / n.d.

1448728_a_at	Nfkbiz	nuclear factor of kappa light polypeptide gene enhancer in B-cells inhibitor, zeta	Mm.247272	2,39	3,57	2,40	0,0016	n.d.
1442340_x_at	Cyr61	cysteine rich protein 61	Mm.1231	2,39	3,66	7,76	0,0048	8
1457823_at	Cyr61	cysteine rich protein 61	Mm.1231	2,36	2,91	5,89	0,0023	8
1416287_at	Rgs4	regulator of G-protein signaling 4	Mm.41642	2,35	3,30	2,80	8,9E-05	3
1418322_at	Crem	cAMP responsive element modulator	Mm.5244	2,33	3,51	3,02	0,0021	1
1451680_at	Srxn1	sulfiredoxin 1 homolog (S. cerevisiae)	Mm.218639	2,32	1,82	1,50	0,0132	n.d.
1419209_at	Cxcl1	chemokine (C-X-C motif) ligand 1	Mm.21013	2,31	3,57	3,19	0,0019	2
1421396_at	Pcsk1	proprotein convertase subtilisin/kexin type 1	Mm.1333	2,28	2,74	2,35	4,6E-04	3
1448471_a_at	Ctla2a	cytotoxic T lymphocyte-associated protein 2 alpha	Mm.30144	2,28	2,31	1,53	0,0125	3
1421679_a_at	Cdkn1a	cyclin-dependent kinase inhibitor 1A (P21)	Mm.195663	2,27	1,74	1,34	0,0206	3
1416431_at	Tubb6	tubulin, beta 6	Mm.181860	2,27	2,42	1,81	3,8E-04	n.d.
1420499_at	Gch1	GTP cyclohydrolase 1	Mm.10651	2,27	1,99	1,64	0,0022	n.d.
1450377_at	LOC640441 /// Thbs1	thrombospondin 1 /// similar to thrombospondin 1	Mm.4159	2,25	2,04	1,78	8,5E-04	n.d.
1451264_at	Frmd6	FERM domain containing 6	Mm.2962	2,24	3,42	2,26	0,0018	n.d.
1453287_at	5730557B15Rik	RIKEN cDNA 5730557B15 gene	Mm.102470	2,23	3,72	2,50	0,0041	3
1427005_at	Plk2	polo-like kinase 2 (Drosophila)	Mm.380	2,23	1,94	1,72	0,0022	4
1453326_at	3300001A09Rik /// EG244	RIKEN cDNA 3300001A09 gene /// predicted gene, EG244911	Mm.105353	2,22	1,52	1,43	5,3E-05	n.d.
1440104_at	Ranbp2	RAN binding protein 2	Mm.401648	2,21	2,85	4,20	0,0211	7
1436329_at	Egr3	early growth response 3	Mm.103737	2,18	3,16	2,50	0,0062	5
1417357_at	Emd	emerin	Mm.18892	2,18	2,72	2,21	4,6E-05	4
1421756_a_at	Gpr19	G protein-coupled receptor 19	Mm.4787	2,17	2,04	1,92	2,5E-04	2
1452418_at	1200016E24Rik	RIKEN cDNA 1200016E24 gene	Mm.332931	2,15	2,23	1,51	0,0034	n.d.
1444402_at	Zc3h12c	zinc finger CCCH type containing 12C	Mm.390172	2,15	1,99	1,41	0,0229	n.d.
1453238_s_at	1200016E24Rik /// 393040	RIKEN cDNA 3930401B19 gene / RIKEN 1200016E24 gene / RIKEN A130040M12 gene / RIKEN E430024C06 gene	Mm.332931	2,15	2,63	1,74	0,0026	n.d.
1424248_at	Arpp21	cyclic AMP-regulated phosphoprotein, 21	Mm.297444	2,14	2,63	2,57	0,0016	n.d.
1422562_at	Rrad	Ras-related associated with diabetes	Mm.29467	2,10	2,59	1,94	0,0006	3
1427539_a_at	Zwint	ZW10 interactor	Mm.62876	2,09	4,68	3,77	0,0227	3
1450716_at	Adamts1	a disintegrin-like and metallopeptidase (reprolysin type) with thrombospondin type 1 motif, 1	Mm.1421	2,08	3,33	3,14	0,0040	3
1415834_at	Dusp6	dual specificity phosphatase 6	Mm.1791	2,07	2,36	2,34	0,0122	2
1422324_a_at	Pthlh	parathyroid hormone-like peptide	Mm.28440	2,06	1,81	1,34	0,0032	3
1429856_at	LOC100048169 /// Tspan1	tetraspanin 18 /// hypothetical protein LOC100048169	Mm.467598	2,05	1,13	1,22	0,0149	n.d.
1435119_at		Transcribed locus	Mm.395027	2,05	1,71	1,26	0,0381	n.d.
1455130_at	Spty2d1	SPT2, Suppressor of Ty, domain containing 1 (S. cerevisiae)	Mm.155687	2,04	3,17	2,92	8,7E-04	n.d.
1460510_a_at	Coq10b	coenzyme Q10 homolog B (S. cerevisiae)	Mm.281019	2,04	2,44	2,15	1,8E-04	n.d.
1423619_at	Rasd1	RAS, dexamethasone-induced 1	Mm.3903	2,03	1,94	1,77	0,0029	6
1437199_at	Dusp5	dual specificity phosphatase 5	Mm.52043	2,03	2,60	2,24	0,0029	n.d.
1416529_at	Emp1	epithelial membrane protein 1	Mm.182785	2,02	3,28	2,79	0,0013	3
1428562_at	2210403K04Rik	RIKEN cDNA 2210403K04 gene		2,01	1,61	1,28	0,0306	n.d.
1422554_at	Ndnl2	necdin-like 2	Mm.19944	2,00	1,53	1,23	0,0390	1
1450708_at	Scg2	secretogranin II	Mm.5038	2,00	2,06	1,82	0,0011	5
1416286_at	Rgs4	regulator of G-protein signaling 4	Mm.41642	1,99	2,93	2,44	1,8E-04	1
1436871_at	Sfrs7	splicing factor, arginine/serine-rich 7	Mm.292016	1,99	2,05	1,90	0,0305	n.d.
1442014_at		Transcribed locus	Mm.441586	1,98	3,66	3,77	0,0054	n.d.
1449227_at	Ch25h	cholesterol 25-hydroxylase	Mm.30824	1,96	2,41	1,61	0,0064	n.d.
1419706_a_at	Akap12	A kinase (PRKA) anchor protein (gravin) 12	Mm.27481	1,95	3,73	2,49	3,1E-04	3
1428923_at	Ppp1r3g	protein phosphatase 1, regulatory (inhibitor) subunit 3G	Mm.473856	1,92	2,97	2,42	0,0186	n.d.
1452519_a_at	Zfp36	zinc finger protein 36	Mm.389856	1,91	2,36	2,39	9,8E-05	4
1424880_at	Trib1	tribbles homolog 1 (Drosophila)	Mm.40298	1,91	2,26	2,13	0,0022	n.d.
1449037_at	Crem	cAMP responsive element modulator	Mm.5244	1,91	2,35	2,31	0,0056	1
1448325_at	Myd116	myeloid differentiation primary response gene 116	Mm.4048	1,90	2,13	2,25	0,0021	3

1428083_at	2310043N10Rik	RIKEN cDNA 2310043N10 gene	Mm.281895	1,90	3,43	2,81	0,0101	n.d.
1434885_at	Spty2d1	SPT2, Suppressor of Ty, domain containing 1 (S. cerevisiae)	Mm.155687	1,90	2,43	2,19	0,0099	n.d.
1418572_x_at	Tnfrsf12a	tumor necrosis factor receptor superfamily, member 12a	Mm.28518	1,88	2,29	1,76	0,0056	4
1443196_at		Transcribed locus	Mm.373919	1,88	2,40	1,57	0,0102	n.d.
1428487_s_at	Coq10b	coenzyme Q10 homolog B (S. cerevisiae)	Mm.281019	1,85	2,53	2,22	2,7E-04	n.d.
1434585_at	Tulp4	tubby like protein 4	Mm.28251	1,84	2,10	1,67	0,0098	n.d.
1417065_at	Egr1	early growth response 1	Mm.181959	1,84	3,27	3,10	7,0E-04	5
1451612_at	Mt1	metallothionein 1	Mm.192991	1,83	1,76	2,12	0,0057	6
1457644_s_at	Cxcl1	chemokine (C-X-C motif) ligand 1	Mm.21013	1,80	2,36	1,90	0,0173	2
1435249_at	Btaf1	BTAF1 RNA polymerase II, B-TFIID transcription factor-associated, (Mot1 homolog, S. cerevisiae)	Mm.295062	1,80	2,30	1,87	0,0030	n.d.
1460275_at	Gpr3	G-protein coupled receptor 3	Mm.4721	1,80	2,34	1,72	0,0013	8
1426081_a_at	Dio2	deiodinase, iodothyronine, type II	Mm.21389	1,79	2,12	1,82	0,0469	3
1448509_at	3110001A13Rik	RIKEN cDNA 3110001A13 gene	Mm.277864	1,77	2,08	1,54	0,0060	1
1428759_s_at	Ccdc49	coiled-coil domain containing 49	Mm.33206	1,77	2,62	2,40	8,6E-05	n.d.
1437481_at	LOC623451	hypothetical LOC623451	Mm.441245	1,73	2,58	2,26	4,8E-04	n.d.
1433582_at	1190002N15Rik /// LOC100	RIKEN cDNA 1190002N15 gene /// hypothetical protein LOC100044725	Mm.258746	1,73	2,04	1,72	0,0042	n.d.
1439826_at	Hspa14	heat shock protein 14	Mm.89341	1,72	2,07	1,94	0,0010	n.d.
1424271_at	Dclk1	doublecortin-like kinase 1	Mm.393242	1,72	2,22	2,05	0,0028	n.d.
1416953_at	Ctgf	connective tissue growth factor	Mm.393058	1,71	2,23	1,69	0,0057	2
1450690_at	Ranbp2	RAN binding protein 2	Mm.401648	1,70	2,03	1,56	0,0062	7
1424107_at	Kif18a	kinesin family member 18A	Mm.274086	1,70	2,42	1,82	0,0267	5
1451289_at	Dclk1	doublecortin-like kinase 1	Mm.393242	1,70	2,17	2,03	0,0090	n.d.
1435248_a_at	Btaf1	BTAF1 RNA polymerase II, B-TFIID transcription factor-associated, (Mot1 homolog, S. cerevisiae)	Mm.295062	1,69	2,49	1,94	0,0151	n.d.
1416892_s_at	3110001A13Rik	RIKEN cDNA 3110001A13 gene	Mm.277864	1,69	2,14	1,78	8,7E-04	1
1446840_at		Transcribed locus	Mm.437560	1,69	2,23	1,51	0,0034	n.d.
1451340_at	Arid5a	AT rich interactive domain 5A (Mrf1 like)	Mm.34316	1,68	2,07	1,70	0,0023	n.d.
1436659_at	Dclk1	doublecortin-like kinase 1	Mm.393242	1,67	2,35	2,07	0,0016	n.d.
1422931_at	Fosl2	fos-like antigen 2	Mm.24684	1,67	2,27	2,16	0,0048	5
1417612_at	Ier5	immediate early response 5	Mm.12246	1,66	2,41	1,80	0,0078	3
1435137_s_at	1200015M12Rik /// 120001	RIKEN cDNA 1200015M12 gene / RIKEN 1200016E24 gene / RIKEN A130040M12 gene / RIKEN E430024C06 gene	Mm.332931	1,66	2,12	1,54	0,0024	n.d.
1434967_at	Zswim6	zinc finger, SWIM domain containing 6	Mm.433838	1,66	2,09	1,54	0,0038	n.d.
1430535_at	Tsc22d2	TSC22 domain family 2	Mm.218409	1,65	2,13	1,75	0,0014	n.d.
1457651_x_at	Rem2	rad and gem related GTP binding protein 2	Mm.274727	1,65	2,06	1,53	0,0045	2
1441894_s_at	Grasp	GRP1 (general receptor for phosphoinositides 1)-associated scaffold protein	Mm.276573	1,64	2,06	1,69	0,0018	3
1422621_at	Ranbp2	RAN binding protein 2	Mm.401648	1,62	2,01	1,71	0,0093	7
1416755_at	Dnajb1	DnaJ (Hsp40) homolog, subfamily B, member 1	Mm.282092	1,62	2,05	2,31	0,0094	6
1435595_at	1810011O10Rik	RIKEN cDNA 1810011O10 gene	Mm.25775	1,62	2,42	1,62	0,0099	3
1456216_at				1,61	2,25	2,43	0,0030	n.d.
1426599_a_at	Slc2a1	solute carrier family 2 (facilitated glucose transporter), member 1	Mm.21002	1,60	2,04	1,61	0,0034	1
1448694_at	Jun	Jun oncogene	Mm.275071	1,60	2,12	2,03	0,0013	4
1449475_at	Atp12a	ATPase, H+/K+ transporting, nongastric, alpha polypeptide	Mm.273271	1,59	2,59	1,92	0,0288	3
1450767_at	Nedd9	neural precursor cell expressed, developmentally down-regulated gene 9	Mm.288980	1,59	2,03	1,34	0,0483	3
1448117_at	Kitl	kit ligand	Mm.45124	1,58	2,01	1,74	0,0143	3
1457167_at	Med14	mediator complex subunit 14	Mm.17616	1,57	2,32	2,04	0,0122	n.d.
1423852_at	Shisa2	shisa homolog 2 (Xenopus laevis)	Mm.275409	1,55	2,24	1,78	0,0058	n.d.
1451415_at	1810011O10Rik	RIKEN cDNA 1810011O10 gene	Mm.25775	1,54	2,33	1,90	0,0125	3
1436202_at	Malat1	metastasis associated lung adenocarcinoma transcript 1 (non-coding RNA)	Mm.298256	1,53	1,84	2,90	0,0338	n.d.
1441536_at	Hmgcs1	3-hydroxy-3-methylglutaryl-Coenzyme A synthase 1	Mm.61526	1,53	2,19	2,31	0,0284	1
1437100_x_at	Pim3	proviral integration site 3	Mm.400129	1,49	2,01	1,89	0,0011	2
1455872_at	BC065085	cDNA sequence BC065085	Mm.37882	1,48	2,28	1,54	0,0066	n.d.

1418681_at	Alg13	asparagine-linked glycosylation 13 homolog (S. cerevisiae)	Mm.249084	1,48	2,34	1,70	0,0122	n.d.
1452521_a_at	Plaur	plasminogen activator, urokinase receptor	Mm.1359	1,48	2,32	1,90	0,0023	0
1433581_at	1190002N15Rik /// LOC100	RIKEN cDNA 1190002N15 gene /// hypothetical protein LOC100044725	Mm.258746	1,47	2,16	1,91	0,0042	n.d.
1430352_at	Adamts9	a disintegrin-like and metallopeptidase (reprolysin type) with thrombospondin type 1 motif, 9	Mm.257557	1,47	2,55	2,41	0,0034	n.d.
1442700_at	Pde4b	phosphodiesterase 4B, cAMP specific	Mm.20181	1,42	2,30	2,52	0,0073	2
1422609_at	Arpp19	cAMP-regulated phosphoprotein 19	Mm.247837	1,42	2,21	2,09	0,0053	2
1425964_x_at	Hspb1	heat shock protein 1	Mm.473688	1,42	2,00	1,94	0,0008	4
1424893_at	Ndel1	nuclear distribution gene E-like homolog 1 (A. nidulans)	Mm.31979	1,39	1,69	2,06	0,0359	5
1457404_at	Nfkbiz	Nuclear factor of kappa light polypeptide gene enhancer in B-cells inhibitor, zeta	Mm.247272	1,34	1,71	2,24	0,0087	n.d.
1455182_at	Kif1b	kinesin family member 1B	Mm.402393	1,28	2,12	1,78	0,0129	n.d.
1418937_at	Dio2	deiodinase, iodothyronine, type II	Mm.21389	1,28	2,19	1,66	0,0124	3
1423422_at	Asb4	ankyrin repeat and SOCS box-containing protein 4	Mm.51340	1,22	2,01	1,39	0,0399	1
1457984_at	Crh	corticotropin releasing hormone	Mm.290689	1,09	3,42	3,47	0,0459	n.d.
1429905_at	Lhx9	LIM homeobox protein 9	Mm.250732	-1,07	-2,10	-1,80	0,0176	1
1423635_at	Bmp2	bone morphogenetic protein 2	Mm.103205	-1,12	2,19	1,87	0,0488	1
1426514_at	4631426J05Rik	RIKEN cDNA 4631426J05 gene	Mm.213582	-1,44	-1,82	-2,04	0,0134	4
1460625_at	Gm1568	gene model 1568, (NCBI)	Mm.29367	-1,48	-2,14	-1,52	0,0116	n.d.
1428682_at	Zc3h6	zinc finger CCCH type containing 6	Mm.26377	-1,55	-2,32	-2,01	0,0023	n.d.
1423146_at	Hes5	hairy and enhancer of split 5 (Drosophila)	Mm.137268	-1,62	-2,39	-1,83	0,0359	3
1456010_x_at	Hes5	hairy and enhancer of split 5 (Drosophila)	Mm.137268	-1,74	-2,54	-1,77	0,0340	3
1455147_at		Transcribed locus	Mm.440042	-1,80	-2,25	-1,95	0,0162	n.d.
1455865_at	Insm1	insulinoma-associated 1	Mm.379070	-1,93	-2,15	-1,93	0,0032	0

Supplementary Table 4

Kainate-induced genes altered in the hippocampus of A-CREB mice at the basal state (Pair-wise significant genes)

FC GCOS = average of fold change control saline vs. A-CREB saline in the two pairs of samples (Batch analysis, GCOS, Affymetrix)

Probe Set ID	Gene Symbol	Gene Title	Unigene ID	FC GCOS	CRE sites
1436387_at	C330006P03Rik	homer homolog 1 (Drosophila) intron	Mm.37533	-1,93	n.d.
1451264_at	Frmd6	FERM domain containing 6	Mm.2962	-1,67	n.d.
1427683_at	Egr2	early growth response 2	Mm.290421	-1,61	3
1418687_at	Arc	activity regulated cytoskeletal-associated protein	Mm.25405	-1,56	2
1422609_at	Arpp19	cAMP-regulated phosphoprotein 19	Mm.247837	-1,56	2
1417065_at	Egr1	early growth response 1	Mm.181959	-1,41	5
1416286_at	Rgs4	regulator of G-protein signaling 4	Mm.41642	-1,32	3
1416287_at	Rgs4	regulator of G-protein signaling 4	Mm.41642	-1,32	3
1422554_at	Ndnl2	necdin-like 2	Mm.19944	1,43	1

Supplementary Table 5: Basal behavior analysis of A-CREB mice

Parameter	Control	A-CREB	p-value
Abdominal Tone	1 (1-1)	1 (1-1)	1
Aggression	0 (0-0)	0 (0-0)	1
Barbering	0 (0-0)	0 (0-0)	1
Body Length (mm)	93.67 ± 1.59	79.17 ± 1.56	**<0.001**
Body Position	2 (2-3)	2 (2-3)	0.27
Contact Righting Reflex	1 (1-1)	1 (1-1)	1
Corneal Reflex	1 (1-1)	1 (1-1)	1
Defecation	2 (1-3)	2 (1-3)	0.84
Fear	0 (0-1)	0 (0-1)	0.58
Gait	0 (0-0)	0 (0-0)	1
Grip Strength	2 (2-3)	2 (2-3)	1
Irritability	0 (0-0)	0 (0-1)	0.32
Lacrimation	0 (0-0)	0 (0-0)	1
Limb Grasping	1 (1-1)	1 (1-1)	1
Limb Tone	1 (1-1)	1 (1-1)	1
Locomotor Activity	12.83 ± 2.12	14 ± 2.09	0.47
Negative Geotaxis	0 (0-0)	1 (1-2)	**0.02**
Palpebral Closure	0 (0-0)	0 (0-0)	1
Pelvic elevation	3 (3-3)	3 (3-3)	1
Piloerection	0 (0-0)	0 (0-0)	1
Pinna Reflex	1 (1-1)	1 (1-1)	1
Provoked Biting	1 (1-1)	1 (1-1)	1
Respiration Rate	2 (2-2)	2 (2-2)	1
Righting Reflex	0 (0-0)	0 (0-0)	1
Seizures	0 (0-0)	0 (0-0)	1
Skin Color	2 (2-2)	2 (2-2)	1
Spontaneous Activity	2 (1-2)	1 (1-2)	0.06
Tail elevation	1 (1-1)	1 (1-1)	1
Toe Pinch	2 (2-2)	2 (2-3)	0.32
Touch Escape	3 (3-3)	2 (1-2)	**0.02**
Transfer Arousal	5 (4-5)	5 (4-5)	0.58
Tremor	0 (0-0)	0 (0-0)	1
Trunk Curl	0 (0-0)	0 (0-0)	1
Urination	0 (0-1)	0 (0-1)	0.26
Vibrissae	1 (1-1)	1 (0-1)	0.32
Visual Placing	2 (1-2)	2 (1-2)	0.52
Vocalization	0 (0-1)	0 (0-1)	1
Weight (gr)	27.8 ± 1.48	18.1 ± 0.58	**<0.001**
Wire Maneuver	1 (0-1)	1 (0-1)	0.92

p-values are calculated using T-test for data expressed as Mean ± S.E.M, and Mann-Whitney test for data expressed as Median followed by Interquartile Range.
Bolded values indicate parameters with significant differences ($p<0.05$)

Supplementary Figure S1

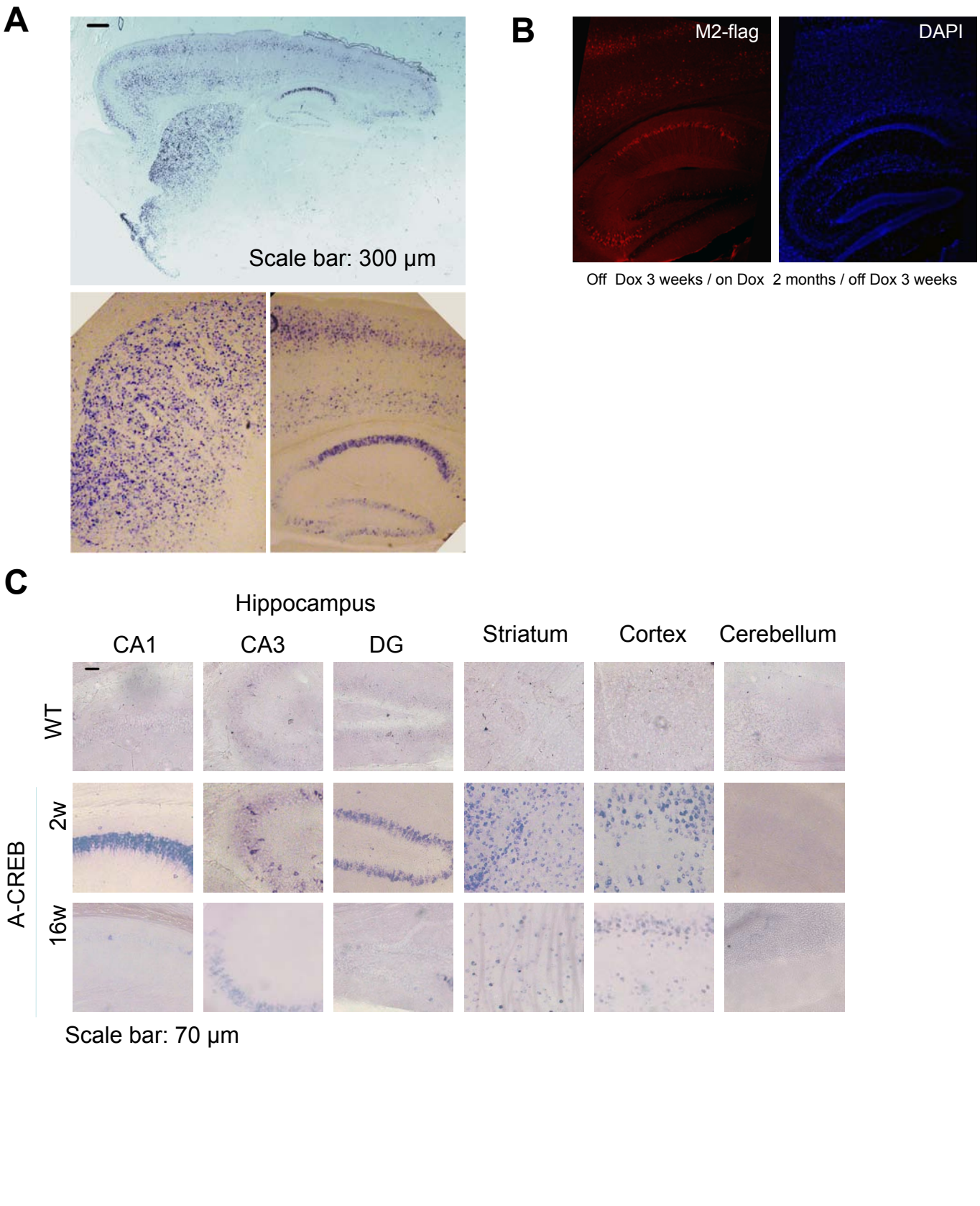

Supplementary Figure S2